

REVIEW OF

State of the Practice Use of Lightweight Cellular Concrete (LCC) Materials in Geotechnical Applications

July 2020

Binod Tiwari, Ph.D., P.E.

Associate Vice President for Research
and Sponsored Projects, California
State University Fullerton

Jeff Wykoff, P.E.

Manager of Geotechnical Solutions,
California Nevada Cement Association

Diego Villegas

Manager of Engineering Fill Division,
Cell-Crete Corporation

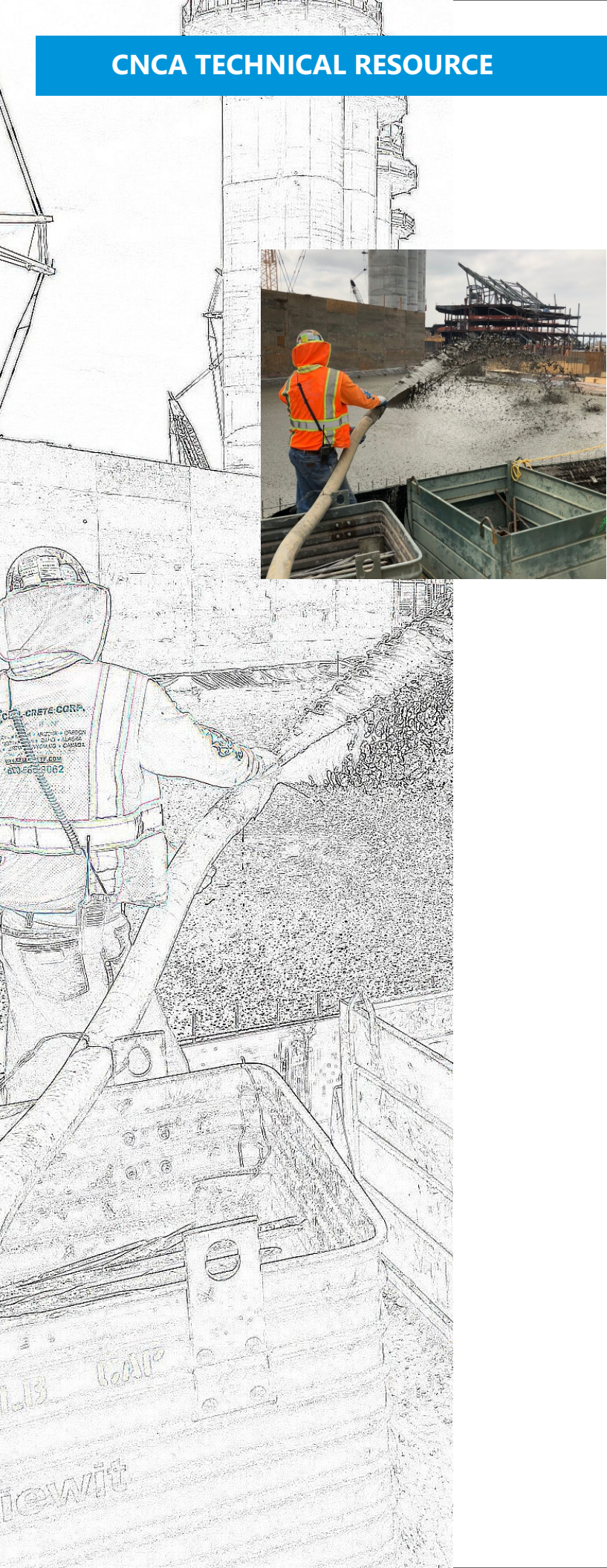


TABLE OF CONTENTS

Contents	Page No.
Abstract	1
Background and History	2
LCC material	3
Properties of LCC Materials	5
Density/Unit Weight	5
Unconfined Compressive Strength	7
Modulus of Elasticity	16
Tensile Strength	18
Flexural Strength	18
Permeability and Saturation	18
Drying Shrinkage	19
Freezing and Thawing Resistance	20
Sorptivity	21
Shear Strength	22
Durability of Concrete	25
At-rest Lateral Pressure (K_0)	26
Stiffness against One-dimensional Consolidation Pressure	27
Poisson's ratio	28
Dynamic Properties	28
Application of LCC Materials	33
Design and Application for Retaining Wall Backfill	36
Case studies	45

ABSTRACT

Lightweight cellular concrete (LCC) has been extensively used globally in various engineering applications for over 60 years. However, its properties have not been well compiled. Moreover, there are limited guidelines available for using LCC materials in geotechnical applications. This study provides an overall summary of the background pertinent to LCC materials, their formation process, including their mechanical and physical properties available in the literature. Moreover, we, in this article, also provide an extensive review on current engineering applications of LCC materials both in civil and geotechnical engineering practice. In this article, we have also included examples of several successful geotechnical engineering applications of LCC materials in the USA with their design approaches and construction details. It is to be noted that this article excludes LCC materials having unit weights greater than 50 lb/ft³ and permeable (PLCC) materials.

BACKGROUND AND HISTORY

Lightweight Cellular Concrete (LCC) also known as Low Density Cellular Concrete or foam concrete or grout has been economically used for various engineering applications such as insulation, and engineering fills. Below grade filling and embankment filling benefits of LCC include efficient production, ease of placement, and quick installation. It has been mentioned in the literature that the patent of the first Portland cement based LCC material was obtained in 1923 by Axel Erikson (Valore, 1954; Ramamurthy et al., 2009; Amran et al., 2015) although lightweight concrete prepared with volcanic ash as fine aggregate has been implemented in civil engineering construction for more than 3,000 years (Tiwari et al., 2017; Maruyama and Camarini, 2015; Chandra and Berntsson, 2003). However, extensive use of LCC in civil, geotechnical or construction engineering projects has only been observed in the past few decades. Application of the LCC material is common in various parts of the world such as Germany, UK, Philippines, Turkey, Thailand, USA, and Canada. Applications include load reduction, load induced settlement reduction, mine stabilization, engineered fills, backfilling of retaining walls, and filling abandoned pipes, tanks and other voids. LCC materials have been identified by various implementing agencies such as California Department of Transportation (CalTrans, 2014) as a method of ground improvement, specifically due to its load reduction capability. CalTrans (2014) has outlined the specifications, and construction considerations for application of LCC materials as lightweight fills (CalTrans, 2014). Detailed review of the history and global application of the LCC materials has been provided by Valore (1954), Ramamurthy et al. (2009), and Amran et al. (2015).

LCC MATERIAL

LCC is defined as concrete made with hydraulic cement, water, and preformed foam to form a hardened material having a oven-dry density of 50 pcf (800 kg/m³) or less (ACI, 2006; ACI, 2014). Although mix-foaming method is also available, pre-foaming method is more common to prepare LCC materials. In the pre-foaming method, preformed foam is prepared by mixing the liquid foam concentrate with water at predefined proportions and then passing this diluted mixture into the foam generator. This preformed foam is eventually passed through specific devices where it gets agitated with the cement-water grout at desired proportion to produce LCC grout and the mixture is then directly placed by hose on the job site (Tiwari et al., 2017). Cements, typically ordinary and rapid hardening Portland cements, calcium sulfoaluminate cement, and high alumina cement, are used as binders. The foam concentrates are mostly prepared with proprietary methods; however, most of them contain protein hydrozylate, glue resins, detergents, resin soaps, saponin, or synthetic surfactants (ACI, 2006; ACI, 2014; Amran et al., 2015). Density of the preformed foam typically ranges between 2.5 to 4 lb/ft³ (pcf). Several chemical admixtures are used in LCC to reduce the amount of water and accelerate setting. Water reducing admixtures help to improve compressive strength of the LCC material. However, it is to be noted that not all chemical admixtures are compatible for use in LCC. Although most of the LCC materials are prepared with preformed foams, cement and water, other Cementous materials such as fly ash, silica fume, high reactivity metakaolin, or ground granulated blast furnace slag are often also added to reduce blending and segregation as well as to increase the compressive strength. Moreover, commercially available fibers such as nylons, polypropylene, polyester, alkali-resistant glasses are also added to increase flexural and tensile strength, impact resistance, fatigue limit, energy absorption and spalling resistance of the LCC material and also to reduce plastic shrinkage cracking of the material after placement. ACI (2014) briefly described the process used for preparing and installing LCC materials. In order to increase the amount of entrained air in the concrete, mixing time is increased; however, over-mixing may reduce the entrained air due to a drop in air contents (Amran, 2015).

Although LCC materials having cast densities larger than 20 pcf is common in practice and can be prepared with the methods explained above, Zhihua et al. (2014) outlined techniques to prepare super low density foamed concrete, with densities ranging from 10 to 19 pcf from Portland cement, chemically developed foams, and admixtures. On the other hand, Hilal et al. (2015) performed an extensive study to evaluate the spatial distribution and size of the air voids and their influence on the compressive strength and other engineering properties of the LCC material. The study was focused on LCC materials having densities ranging from 80-120 pcf. They mentioned that narrower void size distribution shows higher strength. A significant increase in the size of the large air voids can be attributed to large volumes of foams. However, excessive foam volume may result in high amount of void merging, leading to a wide distribution of void sizes and lower strengths. Additives can

help in achieving more uniform distribution of air voids and also in reducing the area of large voids (Hilal et al., 2015).

PROPERTIES OF LCC MATERIALS

Evaluation of the LCC material properties depends largely on application. Quality control of the LCC are generally done with the as-cast density and the corresponding compressive strength of the LCC material. However, several other properties are required to perform appropriate design of the structures made of LCC material. Typical properties of the LCC materials published in the literature are explained in the following sections.

1. Density/Unit Weight

Densities of LCC materials right after its casting (cast density) range from 20 to 120 pcf (Legatski, 1994). Zhihua et al. (2014) were able to produce LCC materials with densities ranging from 10-19 pcf, calling them super low density LCC materials. California Department of Transportation (CalTrans) classified LCC into 6 different categories (Rollins et al., 2019) – a) Class I (cast unit weight ranging from 24 to 29 pcf), b) Class II (cast unit weight ranging from 30 to 35 pcf), c) Class III (cast unit weight ranging from 36 to 41 pcf), d) Class IV (cast unit weight ranging from 42 to 49 pcf), e) Class V (cast unit weight ranging from 50 to 79 pcf), and f) Class VI (cast unit weight ranging from 80 to 90 pcf). Air dry density of LCC material is generally 3-5 pcf less than its cast density. However, the dry density can be up to 10 pcf less than the cast density when they are casted and cured in a low humidity environment (Legatski, 1994). Assuming that a weight of water approximately 20% of the weight of cement is required for the hydration of the cement, Legatski (1994) provided equations for estimating oven dry density of LCC material (D) based on the weight of cement (C in kg/cm³ or lb/yd³) and weight of aggregate (A in kg/m³ or lb/yd³), as presented in Equation 1. As densities of the LCC materials are correlated with other mechanical and dynamic properties, it is important to cast the materials with uniform densities. The cast density of the LCC materials can be varied by changing the amount of cement, water, aggregates, and foamed agent with appropriate ratios.

$$D \text{ in kg/m}^3 = (1.2C + A) \quad \text{or} \quad D \text{ in lb/ft}^3 = (1.2C + A)/27 \quad (1)$$

ACI (2006) and ACI (2014) provide the method to estimate air dry and oven dry density of the LCC materials, based on the as-cast density as presented below in Equations 2 and 3.

$$\gamma \text{ in } \frac{\text{lb}}{\text{ft}^3} = (\gamma_f - 5) \quad (2)$$

$$D \text{ in } \frac{\text{lb}}{\text{ft}^3} = (\gamma_f - 7.8) \quad (3)$$

Where, γ_f = cast unit weight, γ = air-dry unit weight, and D = oven-dry unit weight

Amran (2015) mentioned that the acceptable tolerance in dry density for quality control, expressed in many guidelines, is ± 3 pcf.

Amran (2015) presented relationship between porosity and dry unit weight of LCC material, as presented below in Equation 4.

$$P = 18700 D^{-0.85} \quad (4)$$

where, P = Porosity in %, and D = Dry density in kg/m^3

Wei et al. (2013) developed numerical models and experimentally verified the relationship between air void size and plastic density of the material (Figures 1). The SEM images of the air voids are presented in Figure 2. They developed relationship between target density, foam volume, dry density and unconfined compression strength. Based on the study, they mentioned that air entraining agents introduce large air voids without altering characteristics of fine pore structure of hardened cement paste. When the paste content is less than 48%, average air void size increases significantly as there is not enough cement paste to prevent air void from coalescing. They also observed that the effect of air void on the density is insignificant for the air void size less than 0.1 mm. For LCC material of $2.94 \text{ kN}/\text{m}^3$ (or 18.7 pcf) density, they observed the average pore size to be about 1 mm and most of the pore sizes ranging from 0.75-1.25 mm. Those sizes decrease significantly for higher density cellular concretes (e.g. 0.3 mm for 50 pcf concrete and 0.12 mm for 106 pcf concrete). It is to be noted that although distribution of air-void in the LCC material controls, to some extent, the compressive strength of LCC material, controlling such distribution while manufacturing in batch is very difficult.

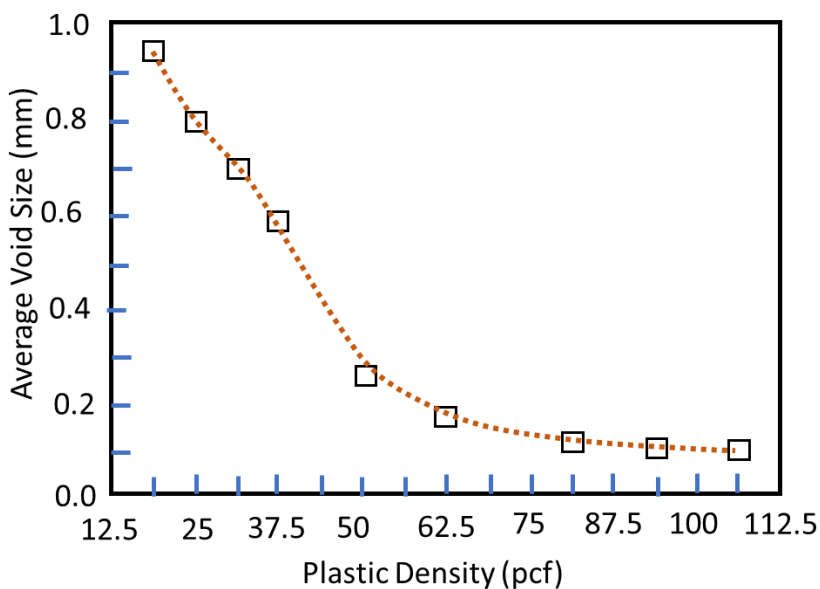


Figure 1: relationship between plastic density and average air-void size (Modified after Wei et al., 2013)

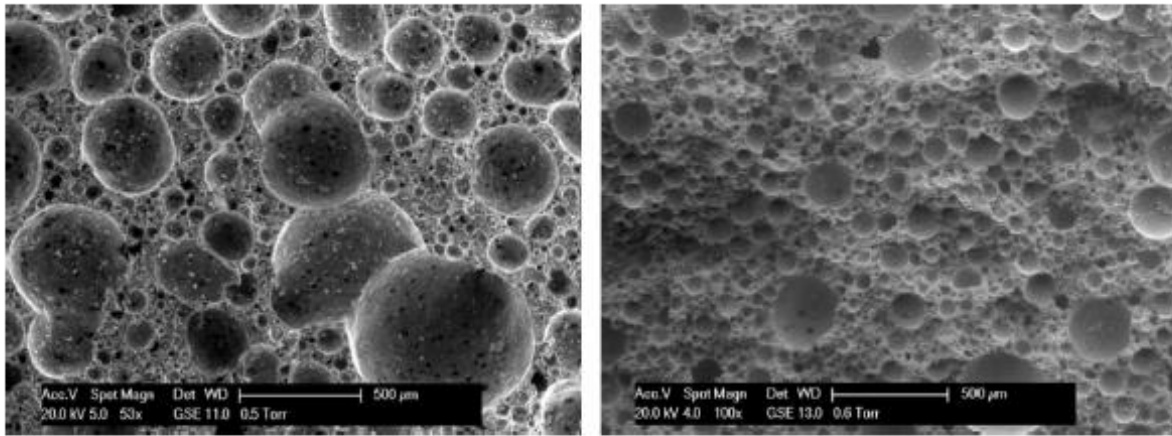


Figure 2: SEM image showing the distribution of air-voids (Copied from Wei et al., 2013)

Hoff (1972) developed relationship between LCC unconfined compressive strength and porosity as well as theoretical paste strength. He mentioned that the porosity includes both entrained and entrapped air as well as capillary porosity. He also developed equation to estimate theoretical porosity with density, water-cement ratio, specific gravity of the cement, and unit weight of water. He conducted experiment to obtain the coefficients developed during theoretical formulation. Through his study, he concluded that the lower limit of cast density from practical consideration is 17.5 lb/ft³.

2. Unconfined Compressive Strength

Unconfined compressive strength (UCS) of the LCC material is among the most published properties. Multiple relationships have been developed to estimate the 28-day unconfined compression strength of LCC material, separately, with cast density, test density at 28 days, and dry density.

Hoff (1970a) measured the UCS of over 800 LCC cylinders with ages up to 471 days by pushing a 4 in diameter piston into a 6 inch diameter and 6 inch tall specimen to measure the UCS of LCC material in the confined condition, which is typical in several practical applications such as tunnel lining. The cylinder was constrained by a 6-inch internal diameter split-wall steel pipe to provide specific confinement to the specimen. Hoff (1970a) recorded yield stress, deformation at yield, average stress between yield strain and 40% strain, and stress at 40% strain and presented specific relationships. He observed that the sample does not exhibit the effect of confinement until the axial strains of 40%, and starts showing high compressive strength afterwards due to the confinement by the steel tube.

Reichard (1970) conducted a series of tests on perlite, vermiculite and cellular insulating concrete to evaluate their mechanical properties. He evaluated the effects of moisture, and size and shape of specimen on compressive strength. He recommended the use of 3 in x 6 in cylinder or 4 inch cube sample for compressive strength measurement. He presented the relationship between wet as well as oven dried density and compressive strength of the tested materials in addition to the relationship between cement content and compressive strength of the materials. He compared the relationship between 3-day, 7-day and 28-day compressive strengths of the tested materials (Figure 3 and 4). Moreover, he also presented the drying shrinkage with time, up to 180 days, and cement contents as well as reduction in moisture with time. Figures 3 and 4 demonstrate that 28-day UCS of LCC is only 5-20% higher than the 7-day UCS. However, 7-day UCS is 40-70% higher than the 3-day UCS.

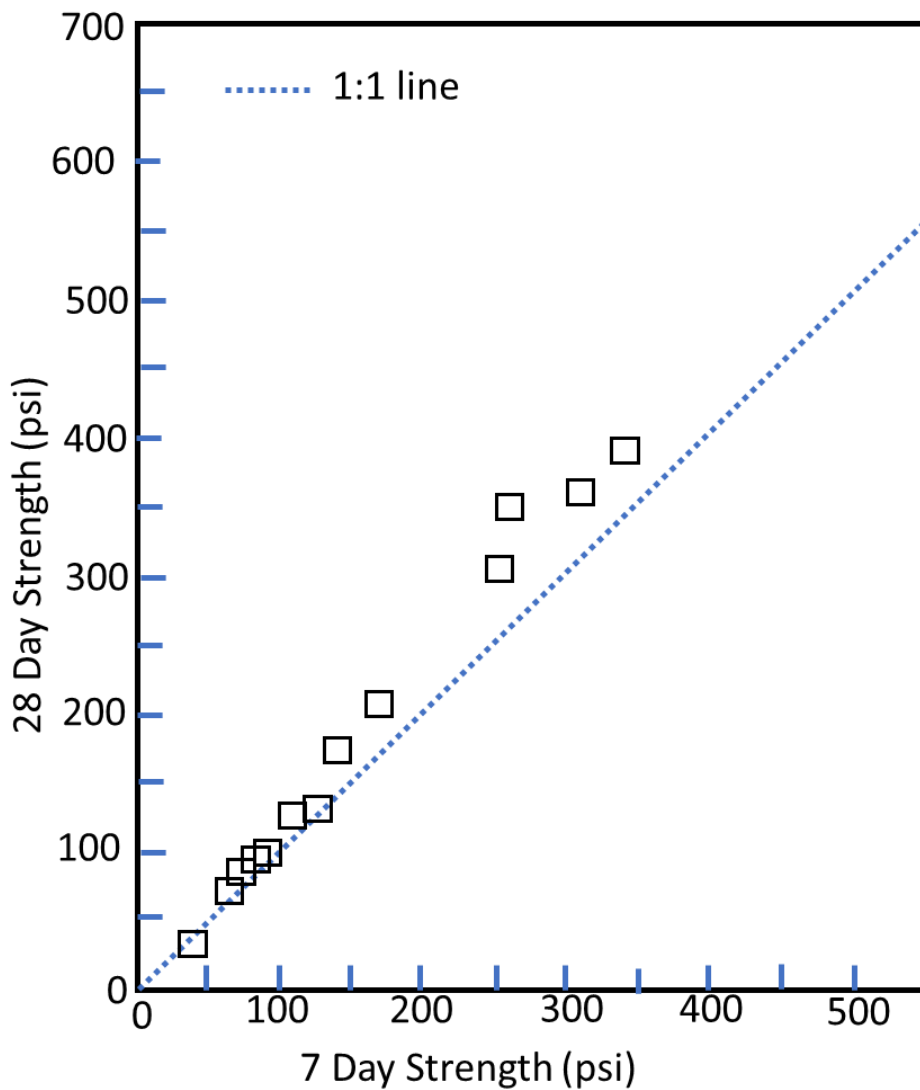


Figure 3: Relationship between 7-day and 28-day compressive strength (Modified after Reichard, 1970)

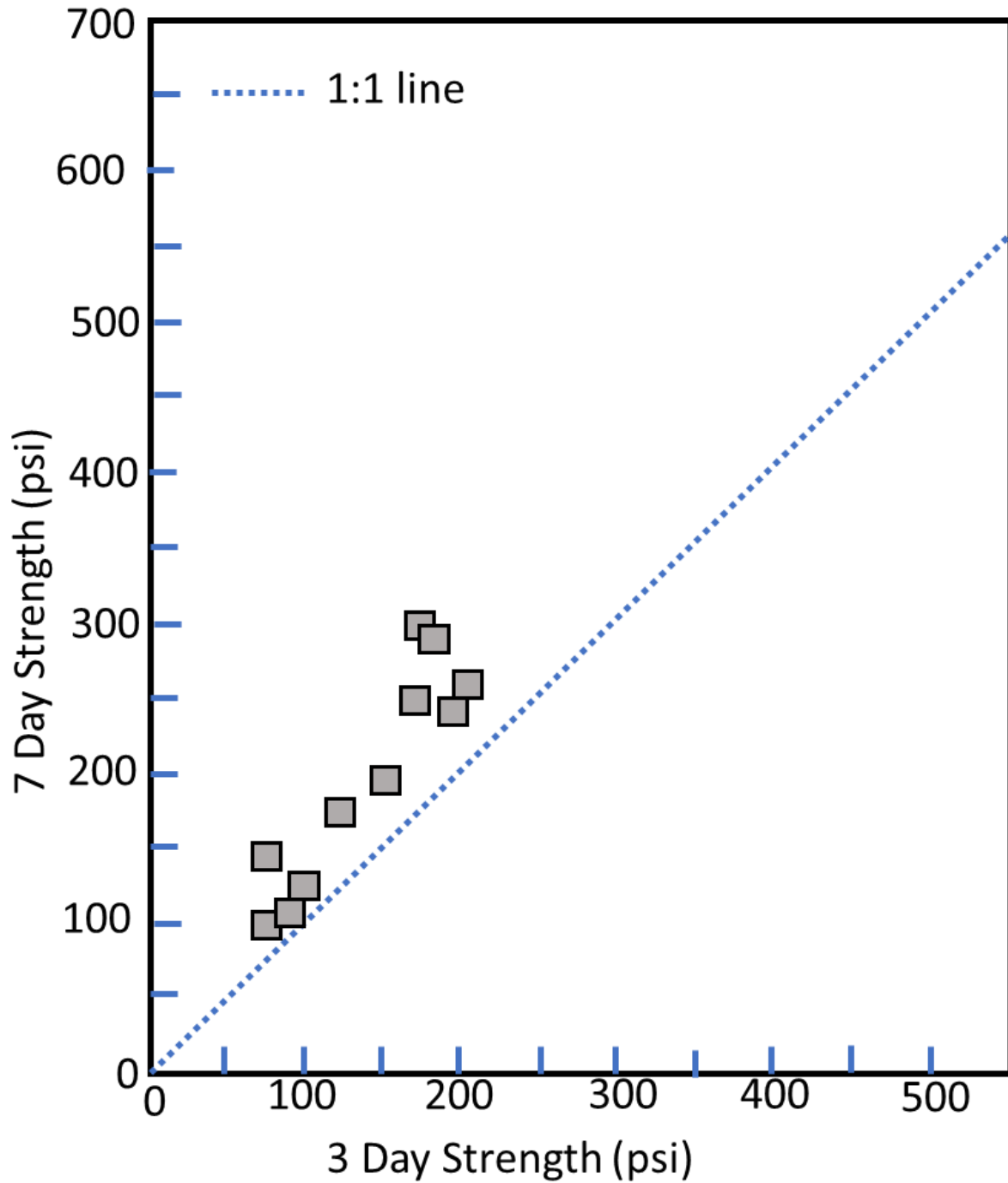


Figure 4: Relationship between 7-day and 3-day compressive strengths (Modified after Reichard, 1970)

Hoff (1972) developed relationship between UCS of LCC material and its porosity as well as theoretical paste strength. In his definition of porosity, he included both entrained and

entrapped air as well as capillary porosity. He also developed empirical equations to estimate theoretical porosity with density for different types of cements tested at different water cement ratios (w/c) by weight, as presented in Figure 5.

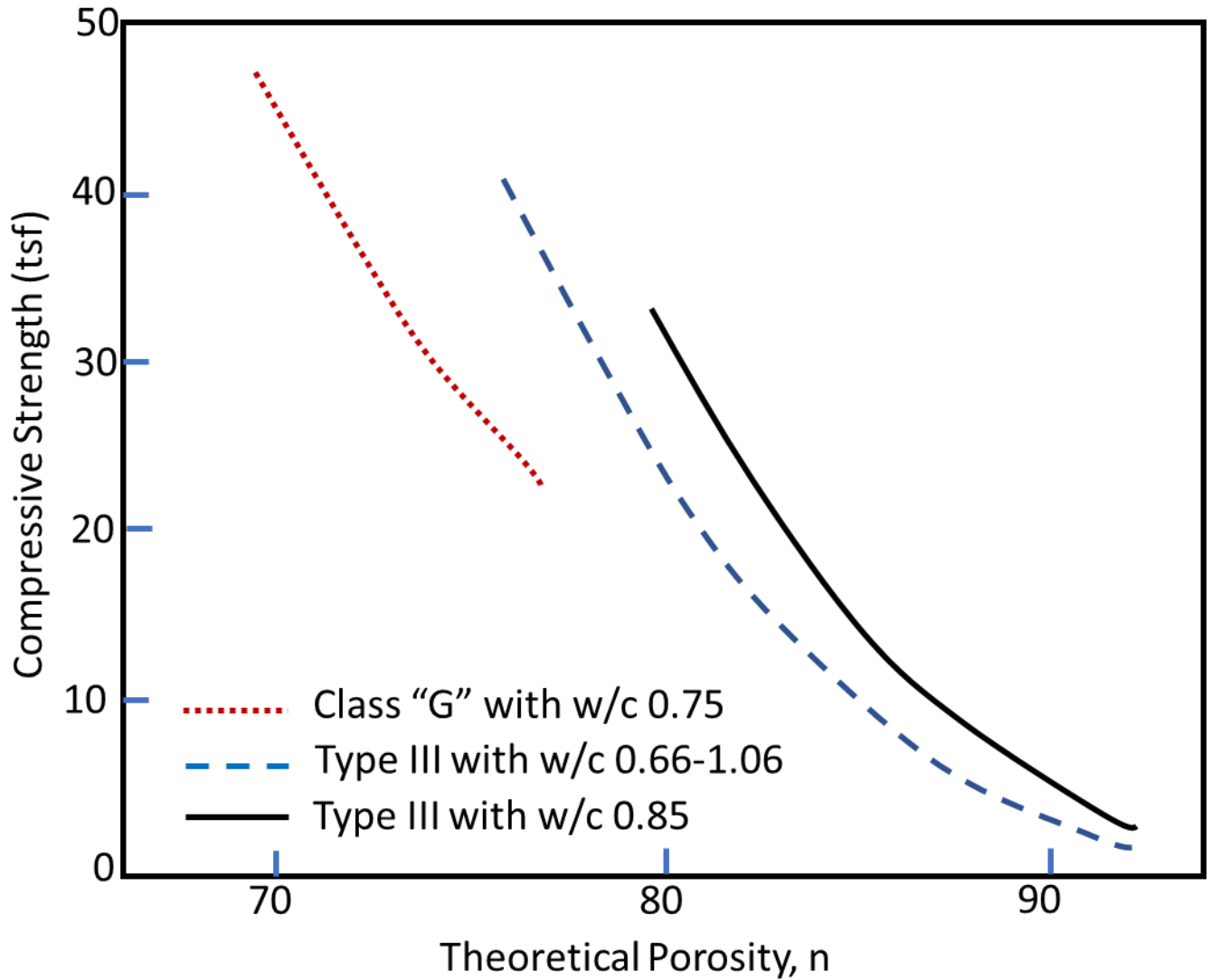


Figure 5: Relationship between theoretical porosity and compressive strength in tons/ft² (tsf) (Modified from Hoff, 1972).

ACI (2006) presented the properties of LCC materials with cast density ranging from 20 to 50 pcf and UCS lower than 1200 lb/in² (psi). ACI (2006) mentions that the relationship between cast density and UCS is an important indicator for quality controlling of the cellular concrete. The compressive strength specimens, as per ACI (2006) and ACI (2014), should not be oven dried as air drying resembles the field condition better. ACI (2006) also mentions that the cast density of the material is usually the most significant property in

many geotechnical applications and is even more important than the UCS. The densities and UCS for LCC materials used in geotechnical application are generally lower than those used for roof deck application. ACI (2006) mentions that introduction of supplementary Cementitious materials including fly ash, silica fume, high reactivity metakaolin, or ground granulated blast furnace slag help to reduce blending and segregation in addition to increasing the strength.

Ramamurthy et al. (2009) conducted experiments to evaluate the UCS of LCC material with respect to the pore size distribution in the concrete material and observed that narrower pore size distribution yielded higher compressive strengths. They mentioned that using fly ash will help in providing more uniform distribution of air-voids as it provides an uniform coating on each bubble to prevent bubble merging. Air bubble merging will cause an increase in pore size and reduction in compressive strength. Specifically, at higher foam volume, merging of air bubbles results into wider distribution of void size which ultimately results in a lower compressive strength. They also observed that the compressive strength of LCC material depends on void to paste ratio, spacing of air voids, and number of air voids. Hilal et al. (2015) also observed similar behavior from their experiments on cellular concrete with densities ranging from 80-120 pcf. Ramamurthy et al. (2009) recommended that the spacing of 0.04 mm, air void size of 0.12 mm, and air content of 42% will provide the optimal combination for high compressive strengths. It was noted that replacement of sand, if is being used, with fly ash increases compressive strength for the LCC material for the same density. Ramamurthy et al. (2009) mentioned that unconfined compression strength of 70 psi is enough for special applications such as pipe and wall insulation, tunnel and mine filling, energy absorption or shock mitigation, and backfill in sewers and highways.

Rahman et al. (2010) performed experiments to evaluate the effect of confinement on the compressive strengths of LCC material. They observed a significant increase in compressive strength of the LCC material with confinement compared to the unconfined specimens. Such increase in UCS is attributed to the fact that the cracked and broken pieces of the brittle LCC after the application of compressive stress during the earlier stage of the test are held within the specimen during the confined tests while they are chipped away during the unconfined tests. This shows that the field compressive strength of the LCC is typically higher than the UCS measured in the lab.

Although the experiments were performed on the cellular concrete with densities ranging from 80-120 pcf, Hilal et al. (2015) observed that air void distribution plays the most significant role on the compressive strength of cellular concrete – narrower void size distribution results in higher strengths. Size of large air voids, according to the observation, increase significantly with an increase in foam volume. They reported that higher foam volume resulted in a greater degree of void merging, leading to a wide distribution of void sizes that corresponded to a lower strength. The study showed that additives help in

achieving more uniform distribution of air voids and also to reduce the area of large voids. They also showed the relationship between wet density, pore diameter and compressive strength of cellular concrete both with and without additives. They observed that D_{90} of pore sizes correlates with compressive strength better than that with D_{50} .

Amran (2015) provided an extensive review pertinent to application and properties of cellular concrete. They mentioned that the compressive strength of the cellular concrete depends on the foam contents and the type of foaming agent as opposed to the water-cement ratio. Although not directly supported with provided literature, they mentioned that the protein-based agent provides a better strength than the use of a synthetic foam agent. Brady et al. (2001) mentioned that protein-based surfactants tend to form a more stable bubbles compared to the synthetics-based ones, giving 45% and 10% higher 28 day compressive strength of LCC for the w/c ratios of 0.35 and, 0.4, respectively than the synthetic-based surfactants. However, considering differences in the density of protein-based and synthetic-based foaming agents, cement content may be different even for the same w/c ratio. As such, direct comparison of the LCC strength with different foaming agents based on w/c ratio is not recommended. Quantity and size of the air bubble have more influence on compressive strength than on the modulus of elasticity. In their extensive review, the authors presented relationships between compressive strength, tensile strength, flexural strength, modulus of elasticity and several other parameters identified in the literature. They mentioned that an increase in the amount of air void reduces the compressive strength of cellular concrete. High strength concrete is generally produced when a water/cement (or binder) ratio of 0.19 (or 0.17) is used. Sand is mixed with cement in some places such as in Europe to increase the strength of concrete. However, for sand-cement ratios higher than 2, influence of sand content is insignificant. Compressive strength of the cellular concrete can be increased by up to 25% using a binary mix of silica fume and fly ash. It was noted that the curing method also influences the compressive strength of cellular concrete. ASTM C-495 specifies the method in detail. Fibers, up to 3% in quantity, can be added to increase the compressive strength of cellular concrete.

To evaluate the effect of drying as well as capping the specimen before testing for the compressive strength of LCC material, ENGEО/CNCA (2016) measured UCS of LCC materials, produced with protein-based foams, for 6 different scenarios including oven-drying – a) oven-dried on 27th day and gypsum capped before testing; b) oven dried on 27th day but uncapped before testing; c) following ASTM C-495 procedure but gypsum capped before testing on 28th day; d) following ASTM C-495 procedure, i.e. samples were not capped before testing on 28th day; e) Moist-curing samples for 29 days and gypsum capping on 29th day before unconfined compression testing; and f) Moist-curing the samples for 29 days but not capping the samples before performing the compression testing on 29th day. The report mentioned that compressive strength reduced by about 10% when samples were uncapped when compared to gypsum capped specimens. It is also reported that the air-

dried specimens provided high compressive strengths compared to moist cured and tested and oven-dried specimens.

Study by Tiwari et al. (2017) is probably the most extensive work in recent years that characterized the mechanical properties of LCC materials, produced with protein-based foams, of different densities commonly used in USA. They compiled properties of Class II, Class IV and other two higher density LCC materials and developed relationships between different densities and other mechanical properties such as UCS (Figures 6-9) as presented in Equation 5. They followed ASTM methods for all tests. They observed that the Class II and IV materials exhibited ductile behavior while materials with cast densities of 45 and 55 pcf were brittle. They also conducted Isotropically Consolidated Undrained (CIU) and Isotropically Consolidated Drained (CID) triaxial tests to evaluate the effect of sample saturation on volume changes during saturation, development of pore water pressure during shearing, as well as undrained and drained compressive strengths. Please note that Figure 7 includes data presented by Hoff (1970a) on confined samples and the data compiled by Legatski (1994). Data presented in Figure 7 suggest that actual laboratory tested values by others are lower than those identified by the empirical relationships established by Hoff (1970a) and Legatski (1994). As the testing conditions and the materials are different than the one used by Tiwari et al. (2017), the results seem slightly different. Likewise, Figure 8 also includes Reichard (1970)'s data points on the data presented by Tiwari et al. (2017).

$$UCS = (291.98 \gamma^2 - 2063.4 \gamma + 3785) \quad (5)$$

Where, γ = test unit weight in kN/m³.

Zhihua et al. (2014) used laboratory mixed chemically foaming process to make LCC of densities ranging from 10 to 19 pcf and measured 3, 7, and 28-day compressive strengths and 28-day water absorption characteristics. They performed experimental laboratory testing to evaluate long-term strength as well as changes in measured strengths of LCC due to different curing process. They observed that steam curing for 12 hours gave almost same strength as 28-day strength. They reported only 3% UCS gain after 1 year of curing compared to 28-day curing.

Amran et al. (2015) provided the following equation (Equation 6) to estimate UCS of LCC material with 7-day compressive strength.

$$f_c = (1.27 f_{c7} + 2.57) \quad (6)$$

where, f_c = UCS in kPa; f_{c7} - 7-day UCS in kPa

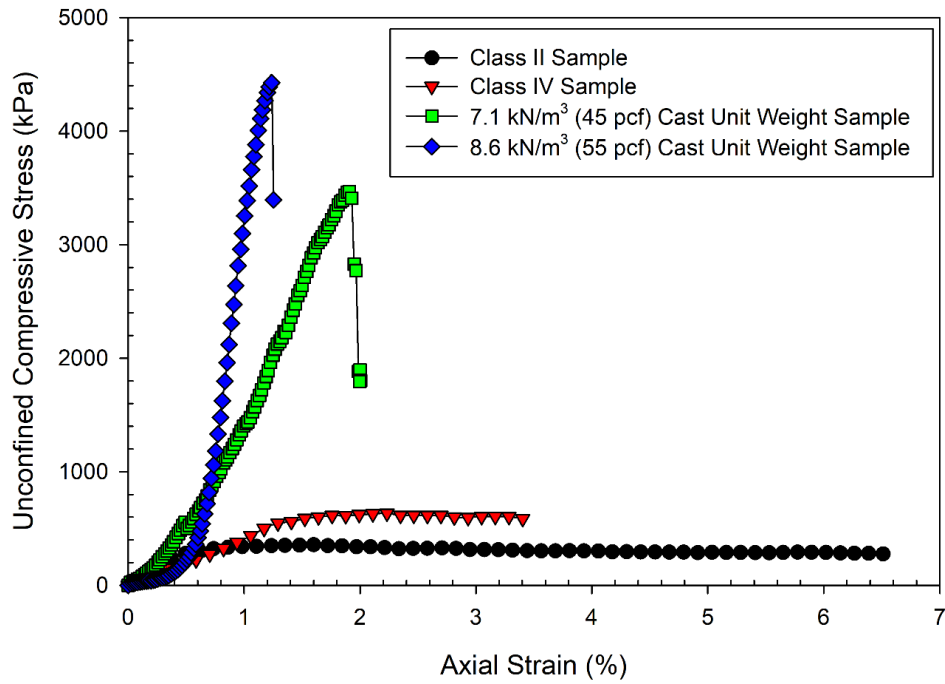


Figure 6: Typical compressive stress-strain curves obtained with uniaxial compression test (copied from Tiwari et al., 2017), note: $f_{tsf} = 95.76$ kPa.

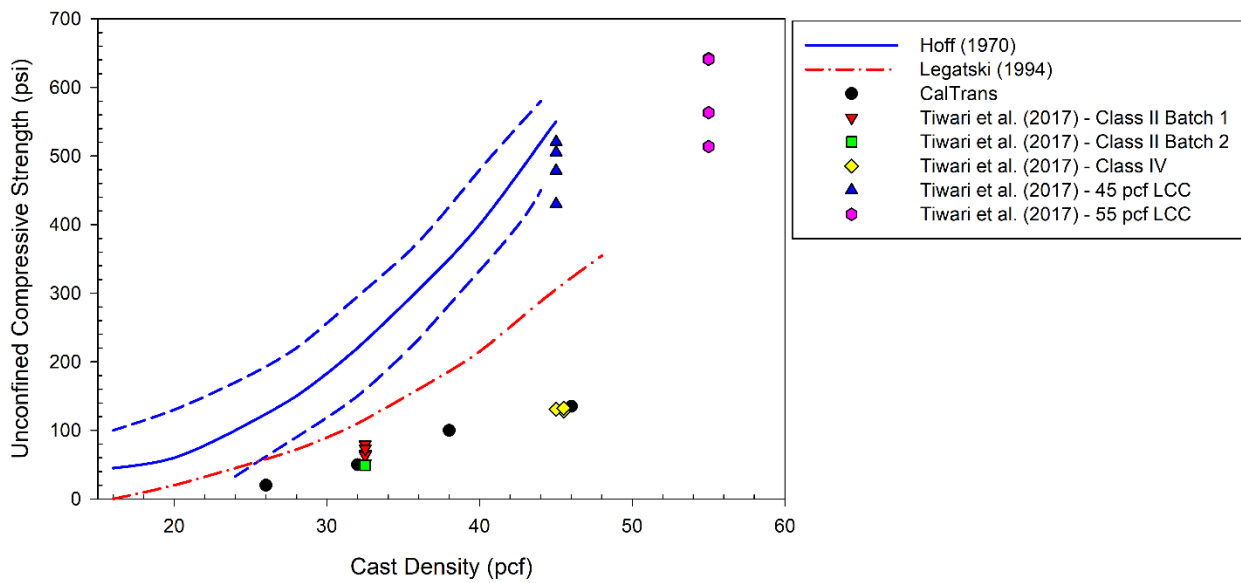


Figure 7: Relationship between uniaxial compressive strength and cast density by different studies. The bands bound by broken lines in Hoff (1970) are the data ranges.

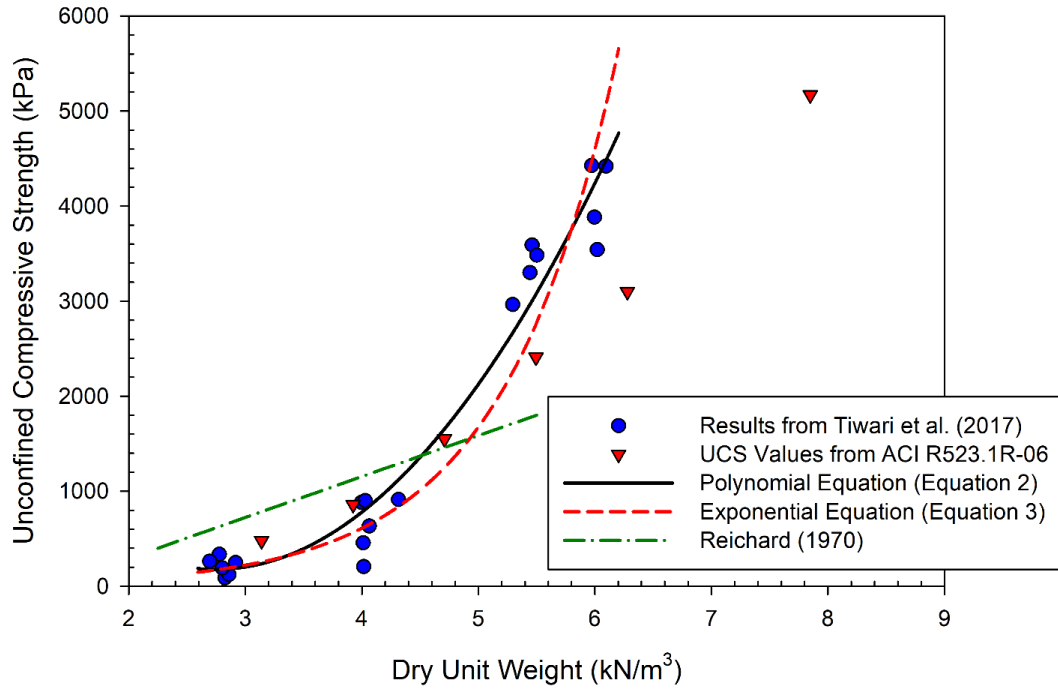


Figure 8: Relationship between unconfined compressive strength and dry unit weight; Note - $1 \text{ kN/m}^3 = 6.366 \text{ pcf}$.

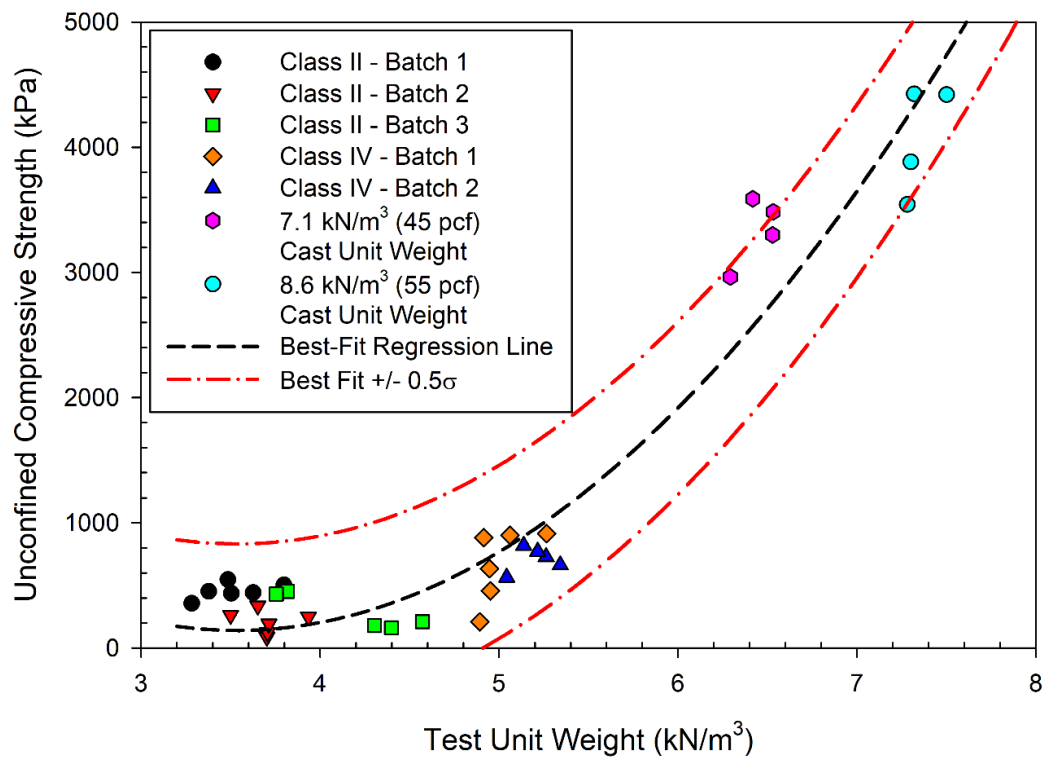


Figure 9: Relationship between UCS and test unit weight (copied from Tiwari et al. 2017)

ACI (2006) compiled the maximum cast density and minimum compressive strength as well as calculated bearing capacity of different groups of LCC materials, as presented in Table 1. Those data were compiled from Engineered Fill, 2011, published by Elastizell Corp. CalTrans, in some of its construction documents, identified those groups as “classes” as presented in Table 1.

Table 1: Maximum cast density, minimum compressive strength and bearing capacity of different classes of LCC materials.

Class	Maximum Cast Density		Minimum Compressive Strength		Bearing Capacity	
	lb/ft ³	kg/m ³	lb/in ²	MPa	ton/ft ²	MPa
I	24	385	10	0.07	0.7	0.07
II	30	480	40	0.28	2.9	0.28
III	36	575	80	0.55	5.8	0.56
IV	42	675	120	0.83	8.6	0.82
V	50	800	160	1.10	11.5	1.10

3. Modulus of Elasticity

To evaluate the deformability of the LCC structure at different applied loads, it is important to understand the Young’s modulus of elasticity of the LCC materials casted at different densities and casting conditions. Modulus of elasticity is also an essential parameter in numerical analyses of structures. Hoff (1970) measured the impact load on the cellular concrete by launching 2.3 lb. cylindrical aluminum projectiles on to a concrete pad and observed that the concrete showed negligible cracking and splitting under the impact load of projectiles in addition to having predominantly plastic failure with little or no rebound. Hoff (1970) mentioned that the unique stress-deformation characteristics of the LCC materials allow these materials to adapt to movements of the confining media without applying large stress distortions to the tunnel liners. Thus, LCC materials offer extensive benefit for their use as backfill for lined tunnels. He mentioned that the crushing strength of an ideal backfill ranges from 100-150 psi and the materials, generally, at this stress deform for strains larger than 40% (Figure 10). Figure 10 also shows the behavior of LCC at varying strains and points of failure. These points suggest a plastic state at relatively large deformation, which is desirable in many geotechnical applications such as seismic design. Such large deformation without crushing of the material can be attributed to the compression of the encapsulated gas in the pore space. Ramamurthy et al. (2009) reported that the modulus of elasticity of the cellular concrete having cast density 31 pcf is about 145 psi. There are several equations proposed in the literature to estimate the modulus of elasticity with cast density and UCS of the LCC material, such as the ones presented below in Equation 7.

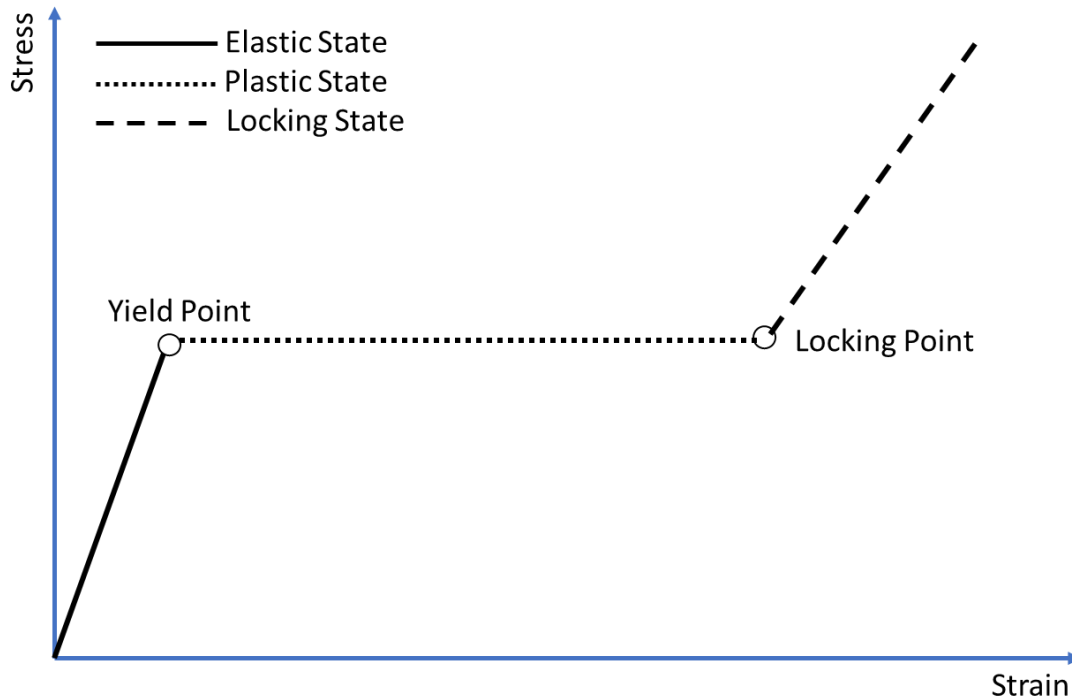


Figure 10: Stress-strain curves for partially confined test (Hoff, 1970a)

$$E_c = \left((W^{1.5})(28.6)\sqrt{f_c} \right) \text{ psi}; \quad (7)$$

W = Cast density – 5 pcf; f_c' = 28 day compressive strength in psi

Legatski (1994) also presented several equations to estimate the modulus of elasticity of LCC material with other properties, as presented below in Equations 8-11.

$$E \text{ in } kN/mm^2 = 5.31 * W - 853; \quad (8)$$

Where, W= density of concrete in kg/m^3 ; and f_c = compressive strength (N/mm^2)

$$E = 33 * W^{1.5}\sqrt{f_c} \quad (9)$$

$$E = 0.42 * f_c^{1.18} \text{ for sand as fine aggregate} \quad (10)$$

$$E = 0.99 * f_c^{0.67} \text{ for fly ash as fine aggregate} \quad (11)$$

ACI (2014) proposed the following equation (Equation 12) to estimate the modulus of elasticity.

$$E \text{ in } psi = 28.6 * \gamma^{1.5}\sqrt{f_c} \quad (12)$$

It is to be noted that LCC unit weights mentioned in ACI (2014) are greater than 50 psi.

Amran et al. (2015) mentioned that the modulus of elasticity of cellular concrete is typically one fourth of the modulus of elasticity of the normal concrete. However, the addition of 0.5% polypropylene fiber (by mix volume) increases the modulus of elasticity significantly. It is more beneficial to add lightweight fly ash than sand to increase the modulus of elasticity.

ENGEO/CNCA (2016) reported that modulus of elasticity of the materials significantly changed, more than 2 times in several samples, when the curing process changed. Moreover, modulus of elasticity of LCC materials tested following ASTM C-495 with gypsum capping were 1.2 to 2.0 times higher than that tested without gypsum capping.

4. Tensile Strength

Tensile strength of the LCC material is also an important parameter for designs pertinent to several geotechnical applications such for seismic loading. Tensile strength of LCC material impacts its resistance, fatigue limit, energy absorption and spalling resistance (ACI, 2006). Legatski (1994) mentioned that the typical values of tensile strength ranges between 10-15% of the compressive strength. However, the tensile strength can sometimes be doubled by adding fibers. The addition of fiber reinforcement was also reported to help reduce thermal cracking in stages of LCC curing. Fiber also help to reduce cracking in early stage of concrete (Amran et al., 2015).

5. Flexural Strength

Flexural strength of LCC material is also as important as the tensile strength for geotechnical application, although the flexural strength of LCC material is not widely reported in literature. Flexural strength of LCC material also impacts its resistance, fatigue limit, energy absorption and spalling resistance (ACI, 2006). Amran et al. (2015) mentioned that the flexural strength of cellular concrete is 0-15% of its compressive strength. However, for LCC materials having density less than 19 pcf, it is negligible. Amran (2015) compiled the equations available in the literature to estimate the modulus of flexural strength of LCC material.

6. Permeability and Saturation

Although proprietary PLCC materials are available in market now, this report deals with the more common (closed cell) LCC. One among the common problems cited for some of the engineering applications of the LCC material is its saturation, although it is less likely

for this material to have a high degree of saturation in its life cycle. LCC materials can become saturated through interconnected voids. Due to the existence of many encapsulated air spaces, the walls of the non-interconnected void spaces have to be ruptured with a large stress for the water to flow through those void spaces, which is less likely in normal situation (Hoff, 1970a). As such, only permeable pores are available for saturation. Compressive stress that the LCC material is subjected to will compress the gases in the pores. If the applied stress is not sufficient to drain the water out, undrained loading prevails; otherwise, if the free water is allowed to escape from the system, unsaturated material behavior prevails (Hoff, 1970a). Hoff (1970a) also mentioned that water pressure as low as 2.5 psi is sufficient to cause free water movement in the LCC materials having densities lower than 35 pcf. However, based on his study, stresses as high as 80 psi maintained for a day were not able to force water through the concrete for the LCC materials denser than 70 pcf. Hoff (1970a) reported that the flow of the water through the cellular concrete erodes the concrete samples. As such, if the concrete is very permeable, it needs drainage provision. Likewise, if the material becomes saturated or partially saturated, pore water pressure developed in the LCC material can increase stress to the walls of porous concrete skeleton, which may eventually be transferred to the facing of the wall, reducing the impact of LCC material as a backfill material. As such, it is important to have proper drainage to prevent a narrow but tall column or wall of water and resulting pressure on the wall. Typically, coefficient of permeability of the LCC material is measured using modified triaxial type tests. ACI (2006, 2014) mentioned that the reported values of the coefficients of permeabilities range from 1×10^{-5} to 1×10^{-6} cm/s. The coefficient of permeability of LCC material increases with an increase in density and decreases with an increase in pore ratio (Ramamurthy et al., 2009). The permeability and degree of fluid flow through the LCC material is a function of large capillary pores rather than total porosity (Amran, 2015). Tiwari et al. (2017) performed extensive study to measure the coefficient of permeability of Type II and Type IV LCC materials and reported that the coefficient of permeability of those materials ranged from 2×10^{-4} to 8×10^{-4} cm/s and 1×10^{-3} to 1.2×10^{-3} cm/s, respectively. However, they also cautioned that reexamination of those values may be needed as these values are higher than the reported values in the literature and that the coefficient of permeability varies slightly with the measurement method. ACI (2014) recommends to use ASTM D2434 for the measurement of the permeability of LCC material. It is to be noted that exact coefficient of permeability is very hard to control in the field while producing the LCC material in a large batch.

7. Drying Shrinkage

ACI (2006) stated that the drying shrinkage of cellular concrete typically ranges from 0.3-0.6% after 6 months and such amount is not critical for applications such as in roof decks and geotechnical applications when compared to structural applications. Figure 11 shows

the variation of drying shrinkage with air dry density of LCC material (ACI, 2006). Due to its high pore content, drying shrinkage potential of cellular concrete is as high as 10 times more than the drying shrinkage potential of normal concrete. However, autoclaving will help to reduce the drying shrinkage by 12.5-50% (Ramamurthy et al., 2009).

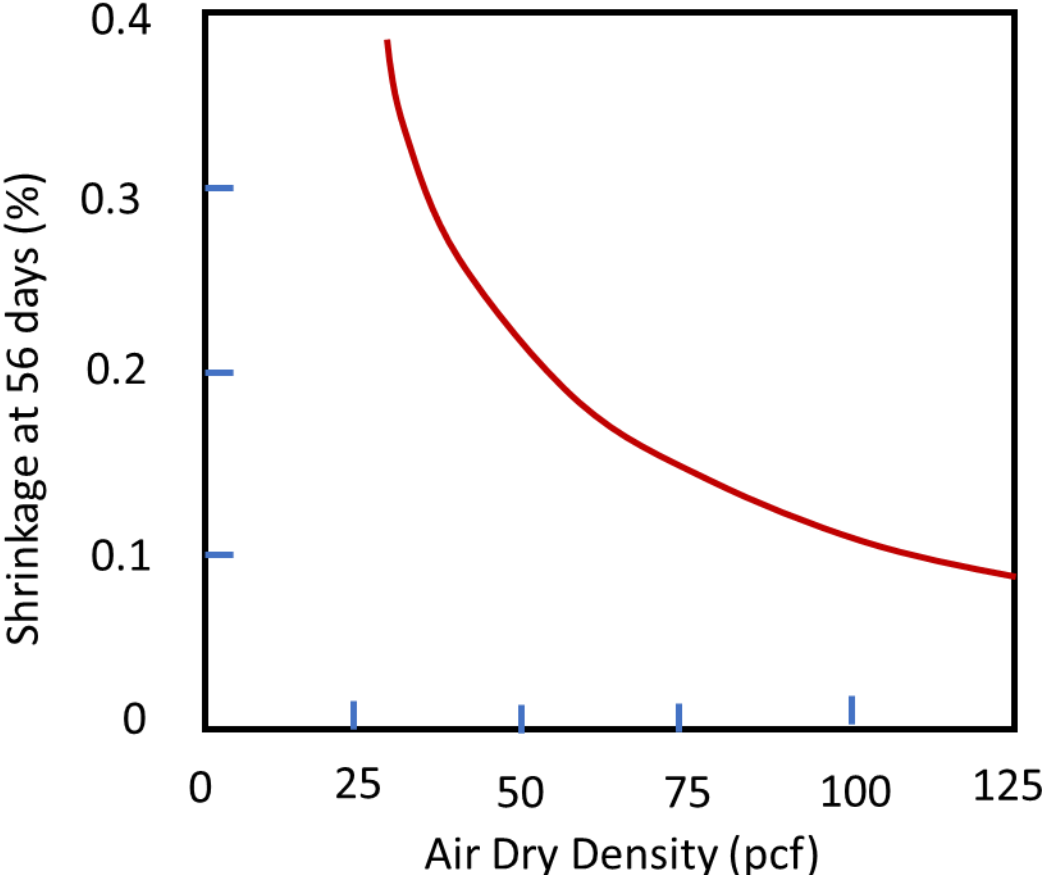


Figure 11: Relationship between air dry density and 56-day shrinkage (Modified from ACI, 2006)

8. Freezing and Thawing Resistance

LCC material have been beneficially applied in areas where there is a high potential of having freeze-thaw cycles. Freezing and thawing of LCC material is measured using Procedure B of ASTM C666 (ACI, 2006). ACI (2006) also mentions that if a LCC material is intended for external exposure to freeze-thaw cycle, it should have a relative dynamic modulus of elasticity at least 70% of its original value after 120 cycles when tested with ASTM C-666 Procedure. Freezing and thawing resistance of the LCC material increases with an increase in its density. As such, LCC materials used within 2-3 ft depth and subjected to freeze-thaw cycles while exposed to water must have a density higher than 36

pcf. ACI (2014) mentions that due to high cement content and extended internal void structure, cellular concretes have very high resistance to freezing and thawing. Volume ratio of reserve pores to critical pores is, generally, used to evaluate freezing and thawing performance of cellular concrete. Figure 12 shows the relationship between moisture content changing with different freeze-thaw cycles.

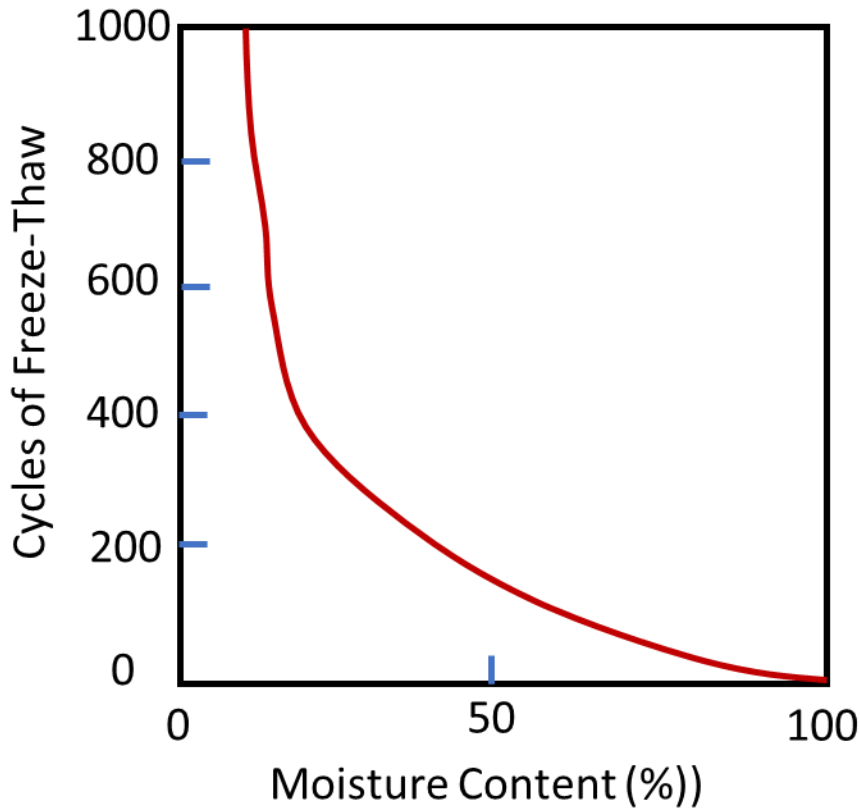


Figure 12: Relationship between moisture content and freeze-thaw cycle (Modified from ACI, 2006)

9. Sorptivity

Sorptivity is defined as the capacity of LCC material to absorb a liquid through capillary action and can be determined through the theory of unsaturated flow. It controls the water movement in concrete. Water movement in LCC materials is not a simple function of porosity, but depends on pore distribution, diameter, continuity, and tortuosity (Amran, 2015). Water absorption and vapor permeability controls the permeability of LCC material. Water absorption of LCC material is as high as two times of that of a normal concrete and does not depend on volume of entrained air and type and contents of ash. Water absorption potential is one among the important properties of the LCC materials for their application

in geotechnical structures. ACI (2014) mentions that fly ash or silica fume can be added in the LCC material to reduce its capillary porosity by reducing water absorption. Amran (2015) presented the empirical models available in literature to estimate sorptivity of LCC material (Equation 13). Legatski (1994) mentioned that if the preformed foam is not tenacious enough to withstand the rigors of batching, mixing and placing, the cell structure of the mixture will interconnect. However high shear mixers are being used these days and the foam is being introduced after the mixing has taken place. This will result in forming channels for high water absorption. Adding fly ash and silica fumes will be helpful in reducing water absorption as their smaller particles will be capable of filling available spaces between cement particles.

$$S = \frac{(\Delta_w)/(A.D_w)}{t^2} \quad (13)$$

Where, S = sorptivity in mm,

t = elapsed time in min,

Δ_w = change in weight ($W_2 - W_1$),

W_1 = Oven dry weight of cylinder in grams,

W_2 = weight of cylinder after 30 min of immersion in gram,

A = Surface area, mm²,

D_w = density of water in kg/m³.

10. Shear Strength

Shear strength of the material is very important for any geotechnical application including application in engineered fill and retaining structures. Legatski (1994) mentioned that the shear strength of LCC material can be calculated from the formula presented in ACI 213R-87. Tiwari et al. (2017) conducted an extensive study to measure shear strength of four different types of LCC materials, widely used in California, using several shear testing devices such as direct shear device (Figure 13), direct simple shear device (Figure 14), and isotropically consolidated undrained (CIU) and isotropically consolidated drained (CID) triaxial tests. Due to the structure of the material, which resembles soft rock, Tiwari et al. (2017) observed high cohesion in all tested LCC specimens (Figure 15). High cohesion in the LCC material can be attributed to cementation (Towerey, 2018) as well as suction (Tiwari et al., 2017, 2018a). Tiwari et al. (2017) developed relationship between test unit weight and cohesion as well as test unit weight and friction angle, as presented below in Equations 14 and 15. The shear stress-normal stress relationships developed with the direct simple shear test for saturated LCC material matched well with that of saturated LCC samples obtained

with CIU and CID triaxial tests. Particularly, the direct simple shear test showed undrained shear strength for saturated specimen with effective cohesion of 5.2 psi and friction angle of 35 degrees, while the CIU and CID triaxial tests also exhibited similar result – effective cohesion of 11.3 psi and friction angle of 34 degrees. Please note that both DS and DSS testing suggests relatively constant strength at high strains consistent with observations by Hoff (1970a).

$$c \text{ in } kN/m^2 = 274.386 * \gamma - 654.958 \quad (14)$$

$$\phi' = 1.187 * \gamma \left(\text{in } \frac{kN}{m^3} \right) + 15.052 \quad (15)$$

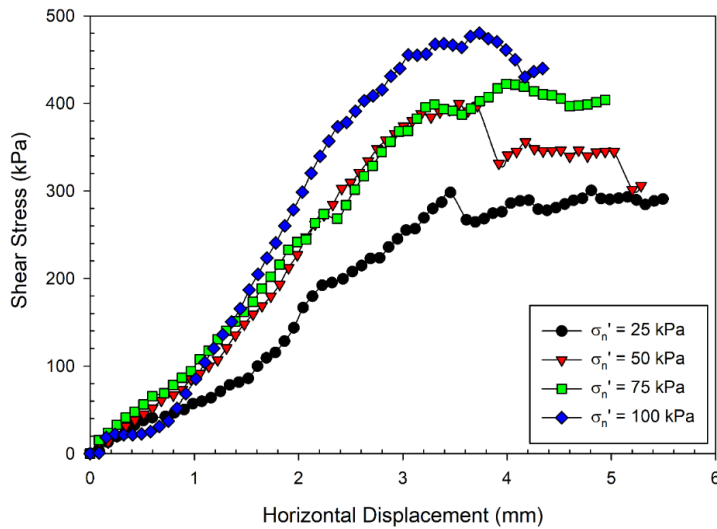


Figure 13: Typical shear stress-horizontal displacement curves obtained from direct shear tests (copied from Tiwari et al., 2017), note 1 inch = 25.4 mm.

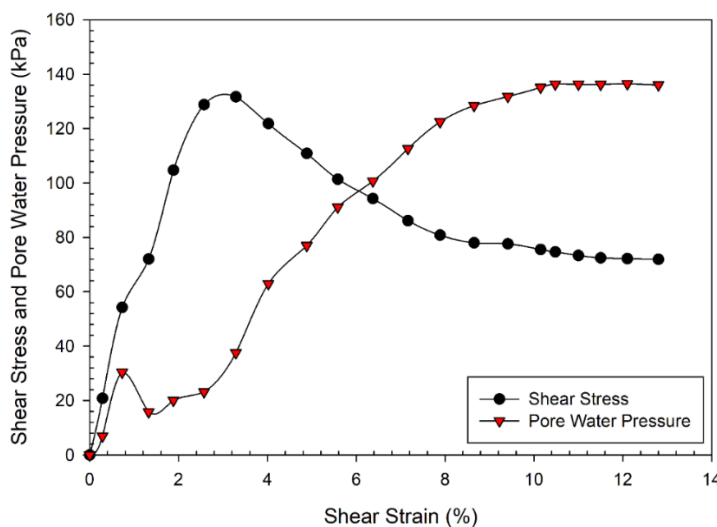


Figure 14: Typical shear stress and pore pressure varied with shear strain in direct simple shear test (copied from Tiwari et al., 2017)

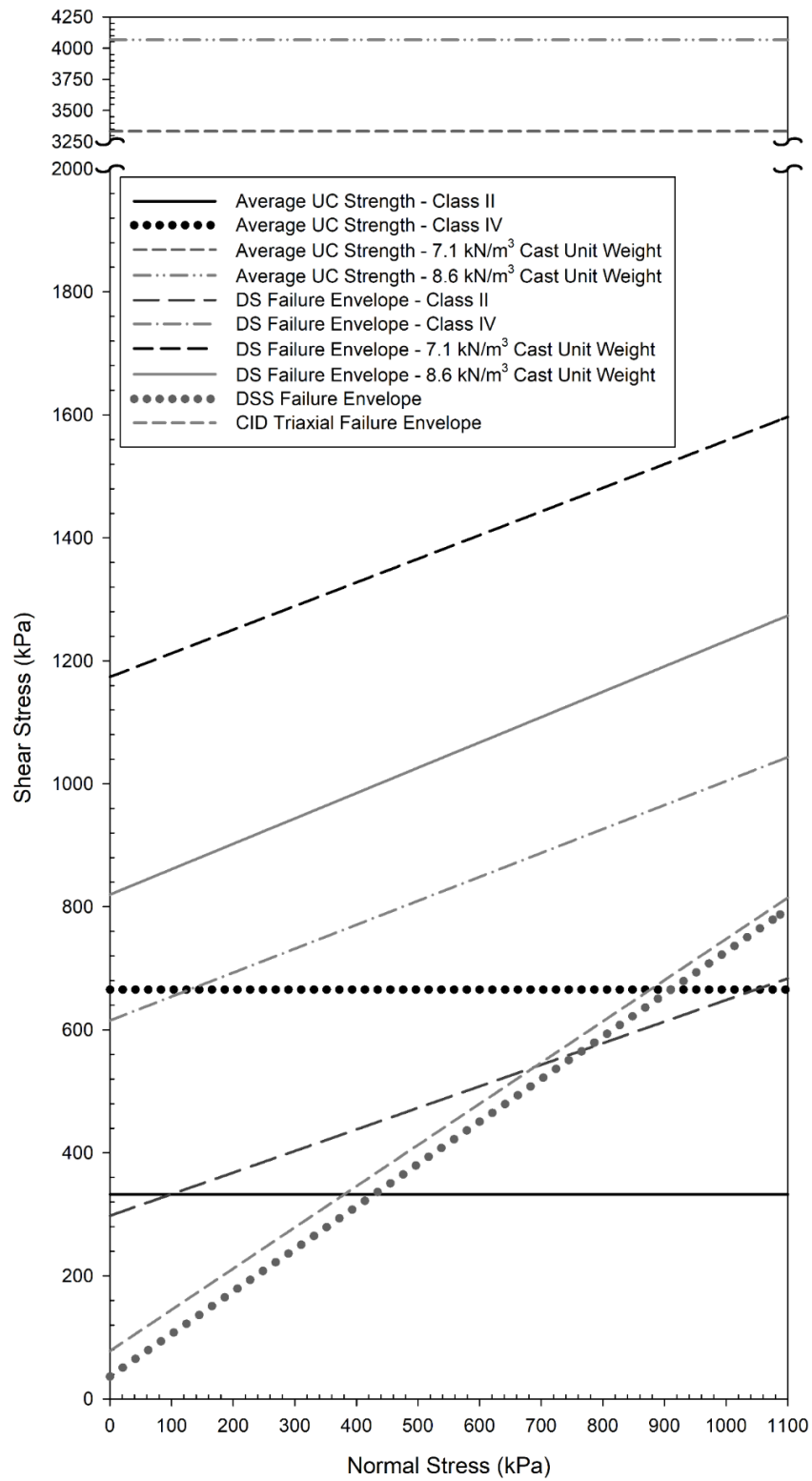


Figure 15: Typical shear envelopes obtained with different test procedures (copied from Tiwari et al., 2017)

11. Durability of Concrete

In general, strength of LCC material is significantly high compared to the soil used in retaining walls and compacted fills of geotechnical structures, specifically due to its high cohesion values. However, it is important to understand its long-term durability and strength loss potential when being exposed to the environment. ACI (2014) mentioned that environmental effects on durability of the LCC materials depends on its initial moisture content. While running laboratory experiments to understand the durability of the LCC material, it was observed that specimens with very high initial moisture content (198%) were destroyed in 5 cycles of alternate drying and wetting cycles whereas the ones with 57% initial moisture contents were severely damaged only after 57 cycles. However, the concrete with 35% initial moisture content demonstrated exceptional performance even after 1500 cycles (ACI, 2014). Durability of the concrete to long-term environment effects has been measured in the past through the permeability and the resistance to an aggressive environment. Environmental degradation of LCC typically depends on size and volume of the pores, their distribution mechanism and mixture composition (Amran et al., 2015). It has been reported in the literature that LCC materials have high resistance to sulfate and carbonate attacks (Amran et al., 2015). Gerhart Cole Inc. (2015) conducted slake durability testing on Type II and IV LCC materials, produced with protein-based foams, following ASTM D 4644 and found that the slake durability index after 2nd cycle ranged from 90-93% (Figure 16).



Figure 16: Slake durability test results after 2 cycles of slaking (Copied from Gerhart Cole Inc., 2015)

12. At-rest Lateral Pressure (K_0)

Tiwari et al. (2017) presented the results of extensive laboratory experiments performed to measure the K_0 value of LCC materials commonly used in USA. They reported that the K_0 values of Class II and Class IV LCC materials generally range from 0.4-0.5 and 0.2-0.3, respectively. It was observed that K_0 values decrease with an increase in the test unit weight of the LCC material (Figure 17).

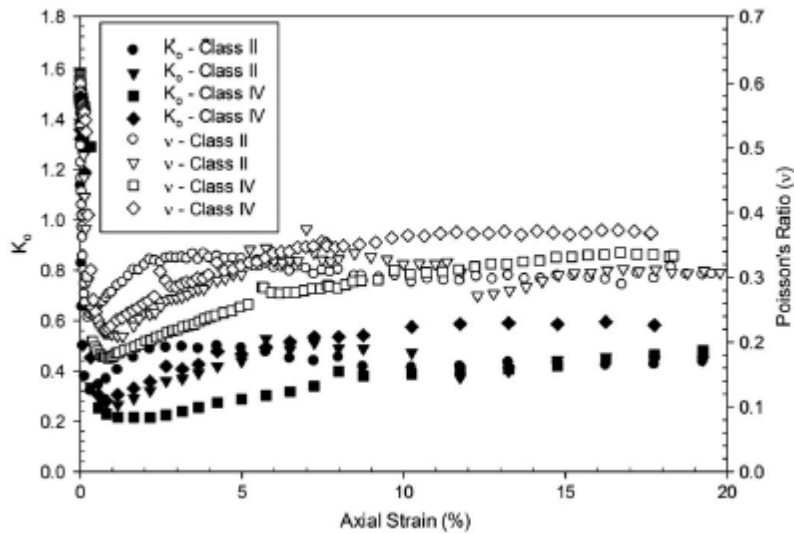


Figure 17: Variation of K_o and Poisson's ratio with axial strain (Copied from Tiwari et al., 2017)

13. Stiffness against One-dimensional Consolidation Pressure

Due to its lightness and the existence of a large portion of encapsulated pores filled with gas, it is important to understand how an increase in vertical stresses can cause deformation of LCC material. Tiwari et al. (2017) explained the experimental details of the 1D consolidation tests performed on Type II and Type IV LCC materials and observed that 1D compression induced deformation significantly increased when normal stresses higher than 300 kPa were applied for Class II LCC materials. Similar high deformation was observed at 700 kPa of compressive stress for Class IV materials (Figure 18). This large deformation at such high compressive stresses can be attributed to the compression of the encapsulated gas filled in the pore space.

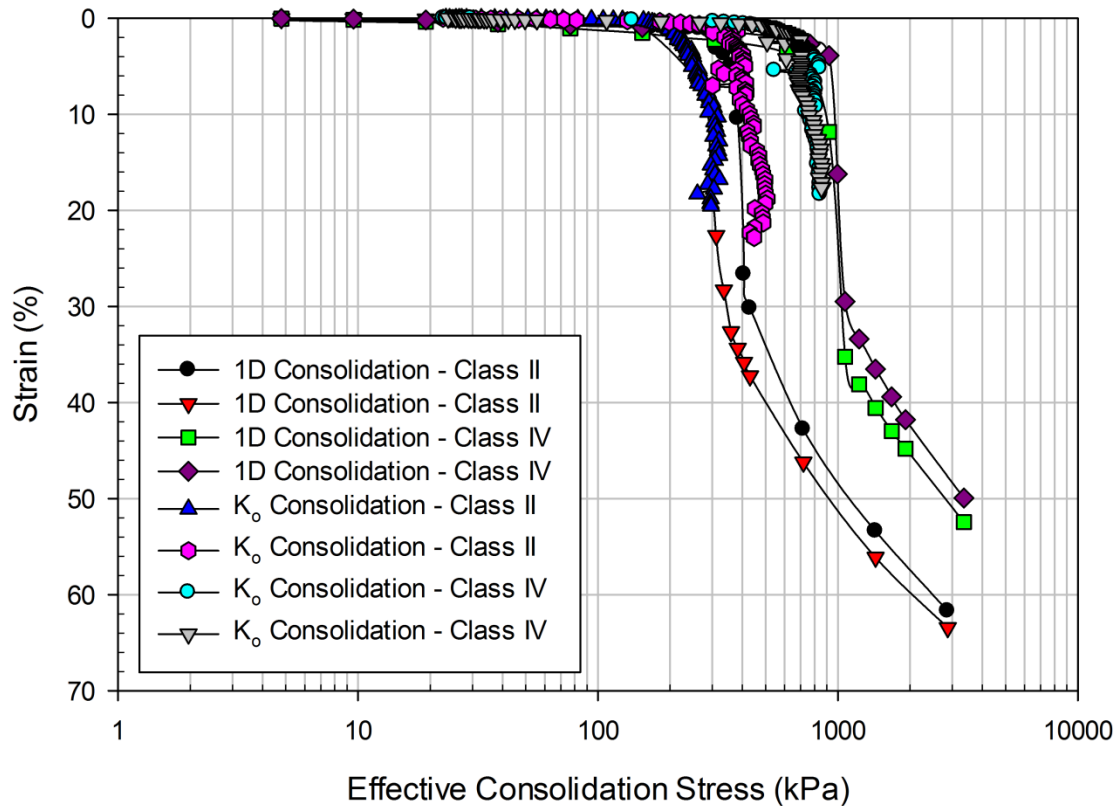


Figure 18: 1D consolidation test results (Copied from Tiwari et al., 2017)

14. Poisson's ratio

To evaluate overall deformation of LCC material upon applied compressive load, it is important to know the Poisson's ratio of the LCC material. Tiwari et al. (2017) performed extensive studies and reported that the Poisson's ratios of both Type II and IV LCC materials ranged from 0.2-0.3. Typical Poisson's ratio for concrete ranges from 0.1-0.2.

15. Dynamic Properties

Dynamic properties of LCC materials are needed to design structures made of LCC materials in seismic regions such as in California. Tiwari et al. (2018) conducted extensive studies to evaluate the dynamic properties of Class II and Class IV LCC materials using the cyclic simple shear device. They also developed stress-strain relationships (backbone curves) from the hysteresis loops obtained from the cyclic simple shear testing (Figure 19). Equation 16 shows the general equation of the backbone curve. Values of a and b in equation 16 depends on the consolidation pressure. The values of a and b are presented in Figures 20 and 21 and Equations 17 and 18, respectively. They reported that the maximum

shear modulus (G_{\max}) decreases with an increase in test density (Figure 22). They also presented the relationship between shear modulus degradation (G/G_{\max}) as well as damping ratios and shear strain for different effective normal stresses (Equations 19 and 20). Based on the results, they observed that G_{\max} increases with an increase in consolidation pressure. Moreover, they observed that the damping ratio reduces with shear strain up to certain shear strain threshold and then increases (Figures 23 and 24). Overall, LCC material shows much larger damping characteristics against seismic loading compared to other geo-materials as well as regular concrete.

$$\tau = \frac{a \cdot \gamma}{b + \gamma} \quad (16)$$

$$a = 0.4593 \sigma_v' \quad (17)$$

$$b = 0.0027 \sigma_v' + 0.0502 \quad (18)$$

$$G_{\max} = 29.48 \sigma_v' + 8110.76 \quad (19)$$

$$G_{\max} = 11955 \gamma + 29400 \quad (20)$$

All G_{\max} , γ and σ_v' are in kPa.

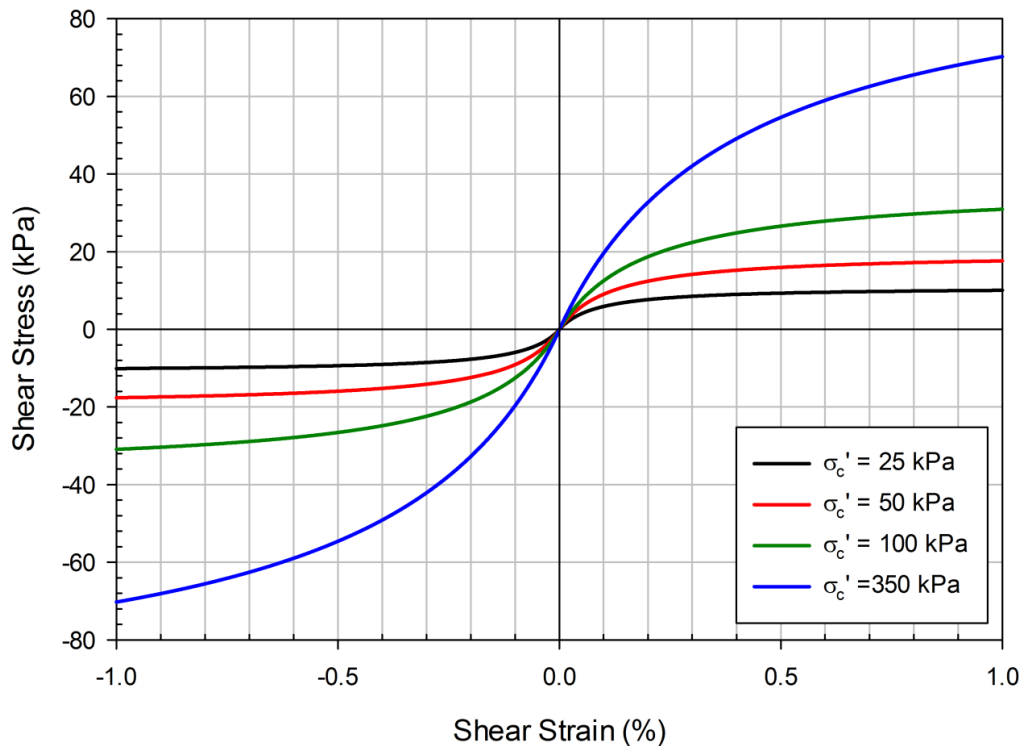


Figure 19: Shear stress-shear strain curve obtained with cyclic simple shear test (copied from Tiwari et al. 2018b)

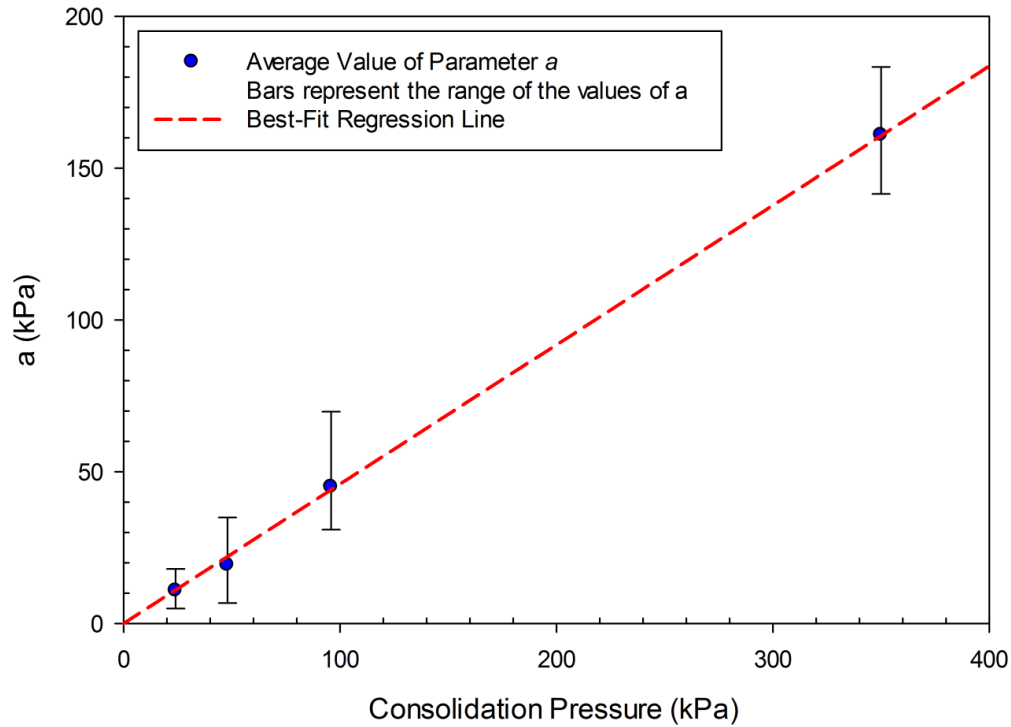


Figure 20: Variation of “a” parameter with consolidation pressure (copied from Tiwari et al., 2018b)

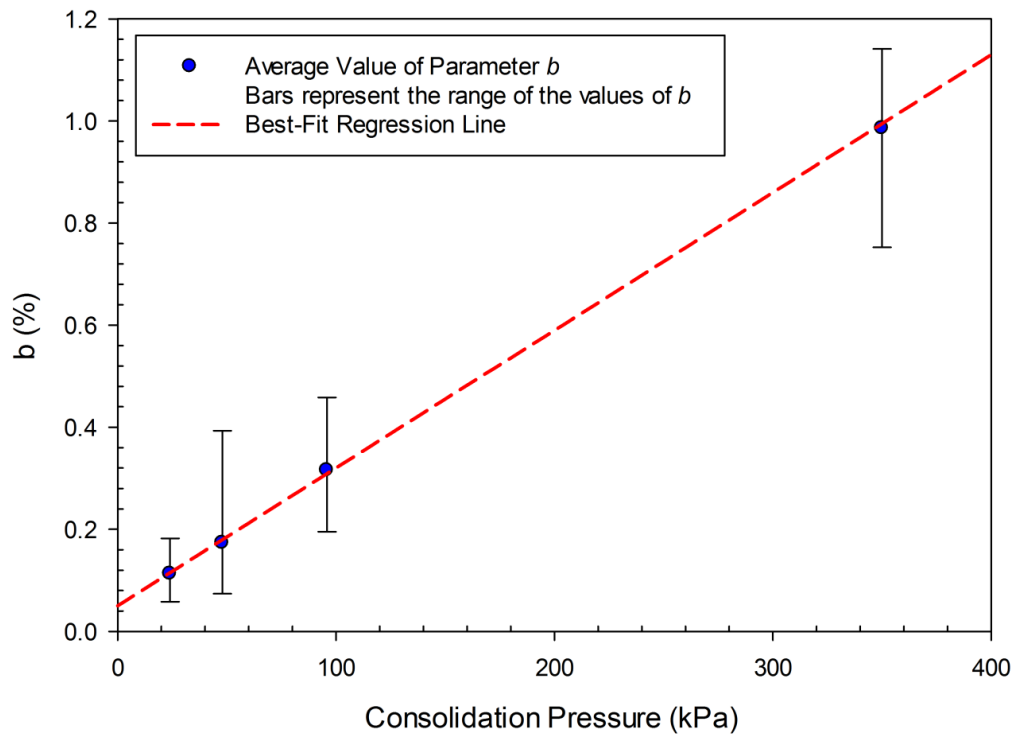


Figure 21: Variation of “b” parameter with consolidation pressure (copied from Tiwari et al., 2018b)

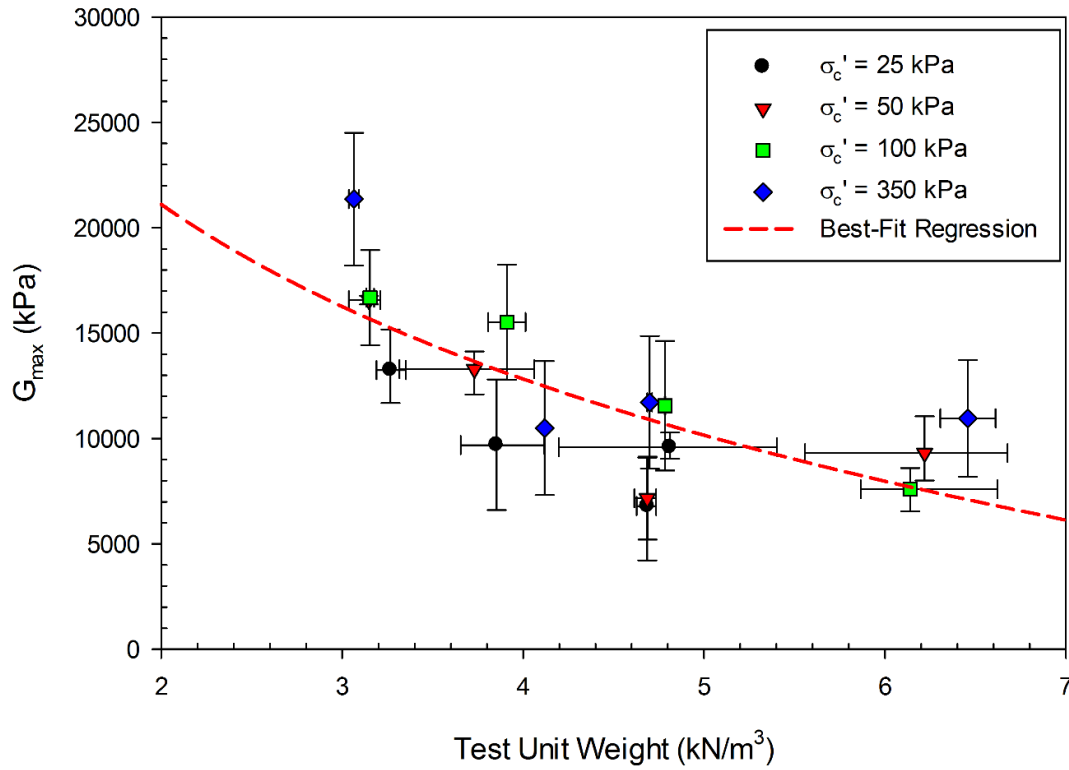


Figure 22: Relationship between G_{\max} and test unit weight (copied from Tiwari et al., 2018b)

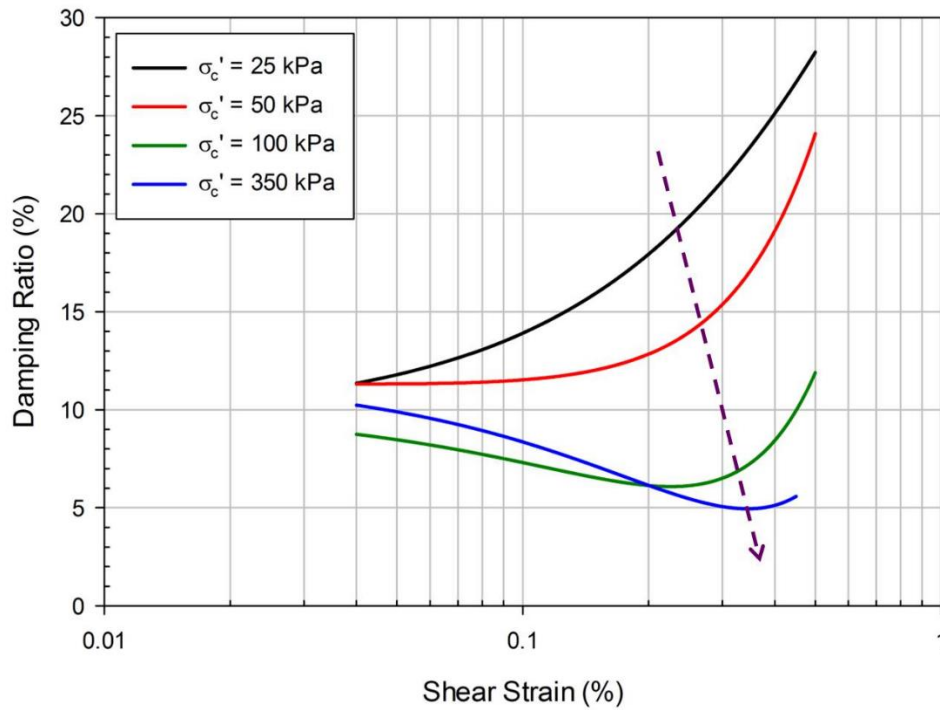


Figure 23: Variation of damping ratio with shear strain for Class II material (copied from Tiwari et al., 2018b)

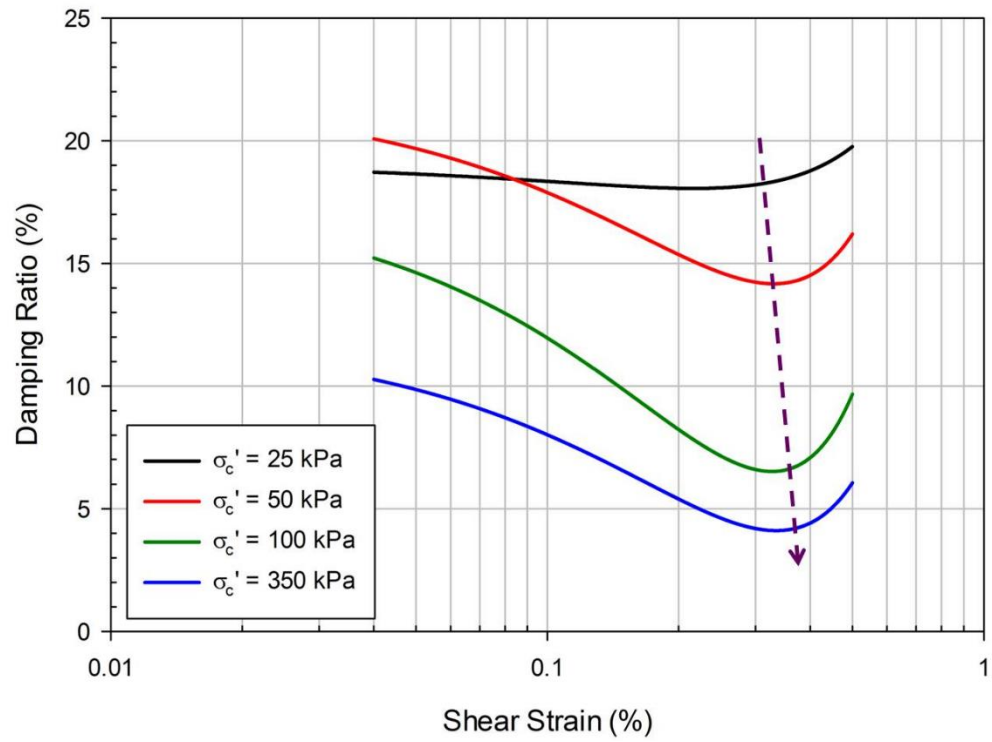


Figure 24: Variation of damping ratio with shear strain for Class IV material (copied from Tiwari et al., 2018b)

APPLICATION OF LCC MATERIALS

LCC materials have been historically used for various engineering applications such as floor fill, roof decks, engineered fills, and precast elements. ACI (2006) mentions that common applications of cast in place LCC materials are on roof decks and geotechnical structures. In geotechnical applications, the material is applied in thick sections with low compressive strengths for the replacement of slightly overconsolidated or normally consolidated or otherwise “poor” soils, fills for abandoned structures such as pipelines and LCC fills designed, mixed and placed to meet specific job conditions and functional requirements. Geotechnical application of LCC material includes backfilling bridge abutments and retaining and building walls as it reduces vertical and lateral pressures. Although ACI (2006) mentions that once the LCC material is set, it does not exert active earth pressure against the wall structure as opposed to standard granular backfills, K_0 values presented above does not concur with the statement presented in ACI (2006). Full scale tests are necessary to confirm the lateral pressure exerted by the LCC wall. Moreover, as it does not require compaction and the settlement is minimal, it is a preferred material in certain circumstances where construction time and ground settlements are a concern. It is also preferred as an alternate to heavy, compacted fills such as in bridge approaches. LCC materials have been extensively used for roadway bases over poor soil. In such applications, the LCC material is cast on the geo-textile that is placed on the completed excavation. Effectiveness of such structures should be verified in future with full scale tests. Likewise, LCC material is a preferred material for pipeline and culvert fills. Placing LCC on both sides of a culvert simultaneously minimizes eccentric loading. ACI (2014) cautioned that for LCC application in cast-in-place vertical walls, forms should be tight and sufficiently strong to resist hydrostatic pressure of the fluid cellular concrete. However, once the concrete is set, lateral pressure on the wall is small. However, full scale tests are needed to conform the lateral pressures exerted by the LCC structures. Moreover, for fill materials under standing water, it is recommended to use cellular concrete heavier than 65 pcf (ACI, 2014). It is to be noted that extra precautions, admixtures, and tremie placement may be required for more challenging placements in water. Dewatering may be a preferred solution. Placement of LCC should not proceed in flowing water conditions. Water should be removed for annular space grouting,

CalTrans mentions that LCC provides a method for ground improvement (CalTrans, 2014). CalTrans (2014) provides specifications for lightweight fills and design methods for the LCC in addition to specification and construction considerations.

Other than the applications explained above, there are several other applications of the LCC materials, such as, shock-absorber and backfill for lined tunnels. Hoff (1970b) studied the potential of using LCC material as a shock absorbing backpacking material outside buried structures or bunker tunnels to provide protection from explosive fragments, high impact shots or explosions (Figure 25). LCC material showed negligible cracking and

splitting under impact load of projectiles and had exhibited predominantly plastic failure with little or no rebound. From the experimental results, they observed that LCC materials can effectively be used for backpacking of the protective structures as a shock absorber. Please note that backpacking is installed around a structure as shock absorber and is not a backfill.

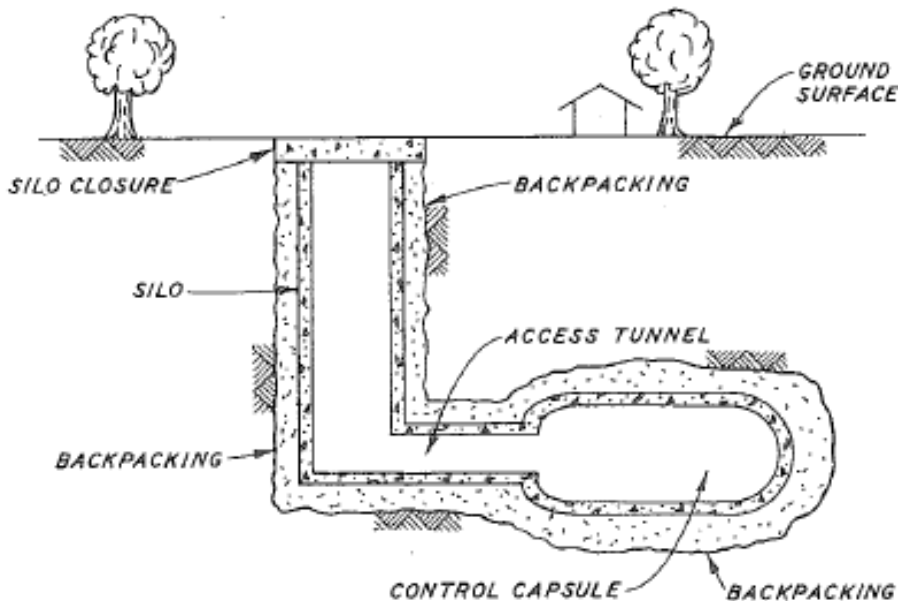


Figure 25: Test set up of Hoff (1970b) to evaluate the suitability of LCC material as shock absorber (copied from Hoff, 1970b)

Hoff (1970a) performed extensive laboratory experiments to evaluate the potential of LCC material as the backfill of lined tunnels. He reported that due to their unique stress-deformation characteristics that allow them to adapt to movements of the confining media without applying large stresses distortions to the tunnel liners, LCC materials can be beneficially used as backfill for lined tunnels. He also noted that the ideal backfill can have a crushing stress around 100-150 psi and will deform at that crushing stress for strains larger than 40%. He mentioned that the deformation at such situation is mainly due to the compression of the encapsulated gas in the pore space.

One of the concerns raised in the literature regarding installation of the LCC material is elevated temperature right after the pouring. Hoff (1970b) performed extensive studies and presented a report on how temperature changes right after the installation (Figure 26) at top, middle, and bottom of the lift. Such temperature variation also depends on the type of cement and the lift thickness. Cell-Crete Corporation (private communication) noted

approximately 205°F rise in temperature at the middle of the lift after 12 hours of placement, which dropped to approximately 100°F after 50 hours of installation. Within one lift, maximum temperature was recorded at the center of the layer and the lowest was recorded at the top of the layer.

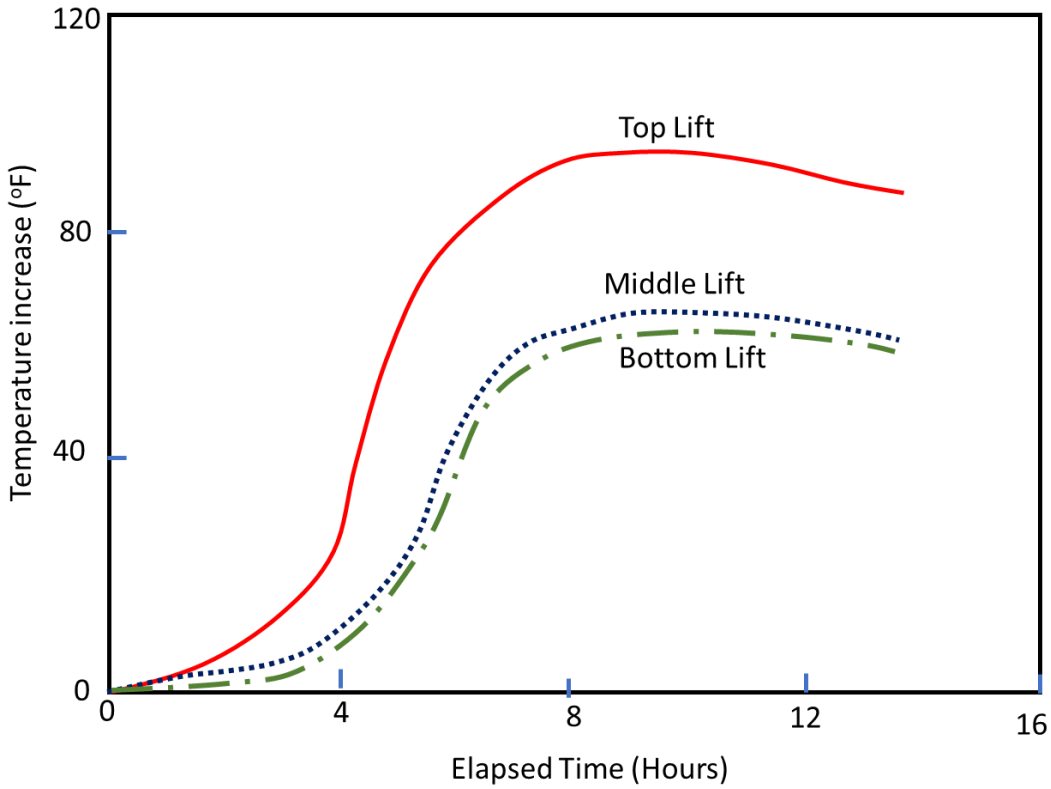


Figure 26: Increase in temperature during concrete hydration process for Type I Cement (modified from Hoff, 1970b)

DESIGN AND APPLICATION FOR RETAINING WALL BACKFILL

Although LCC materials have extensively been used in retaining walls and engineered fills, there is very little information available in the literature regarding the engineering parameters and design methods of such applications. Nonetheless, there are a few articles that demonstrate the successful application of LCC material in retaining walls.

One concern while designing with pre-cast panels typically used for mechanically stabilized earth (MSE) walls, but using LCC fill is the appropriate value of drained friction angle of the material to be used in the calculations. Tiwari (2015) and Tiwari et al. (2017, 2018a) mentioned that in general, MSE walls made from LCC material should be free-standing after curing. However, as the current MSE wall design guidance and methods in USA require using the friction angle of backfill material, they proposed to use the friction angles of 35° for short-term and 40° for long-term conditions. They also mentioned that these values are highly conservative as they do not foresee the LCC materials will be completely saturated in their life period. Towery (2018) discussed that free-standing property of LCC material is permanent, not temporary as there had been no issues observed for thousands of applications nationwide in USA and Canada. The cracks, if developed in the LCC retaining walls, are due to shrinkage and creep as opposed to loading stress and do not have any adverse effects on the performance of the walls.

Pradel and Tiwari (2015) performed numerical analysis on a 23 ft tall MSE wall made of LCC material founded on soft ground under seismic loading condition. They used the dynamic and static strength properties mentioned in Tiwari et al. (2017, 2018b) in their numerical analysis. Their numerical analyses demonstrated that the retaining wall (mentioned in their report as MSE wall) moved monolithically under seismic loading. The analysis suggested that the seismic loads taken by the geo-grid reinforcement was transferred immediately to the LCC material. As such, geo-grid did not have much role other than preventing crack propagation.

Tiwari (2018) and Tiwari et al. (2018c and 2018d) performed over 20 shake table tests on LCC block with geo-grid at the center to evaluate the performance of the geo-grid and LCC material during seismic loading (Figures 27 -29). The blocks were inserted into several steel dwellings projected up from the shake table to ensure full attachment of the blocks with the table. They observed that the LCC block moved monolithically with no significant difference in deformation between the geo-grid reinforcement and the LCC and also from top to the bottom of the block (Figure 30) although the displacement records between the table and the block were slightly out of phase which could have been due to experimental set up. They applied two different surcharge loads (0.72 psi and 1.16 psi) to mimic two different heights of the wall and found results similar to those explained above in both models.



Figure 27: Geo-grid reinforced LCC block tested by Tiwari et al. (2018c and 2018d) on shake table, tested at surcharge pressure of 0.72 psi (copied from Tiwari et al. 2018c and 2018d)



Figure 28: Geo-grid reinforced LCC block tested by Tiwari et al. (2018c and 2018d) on shake table, tested at surcharge pressure of 1.16 psi (copied from Tiwari et al., 2018c and 2018d)

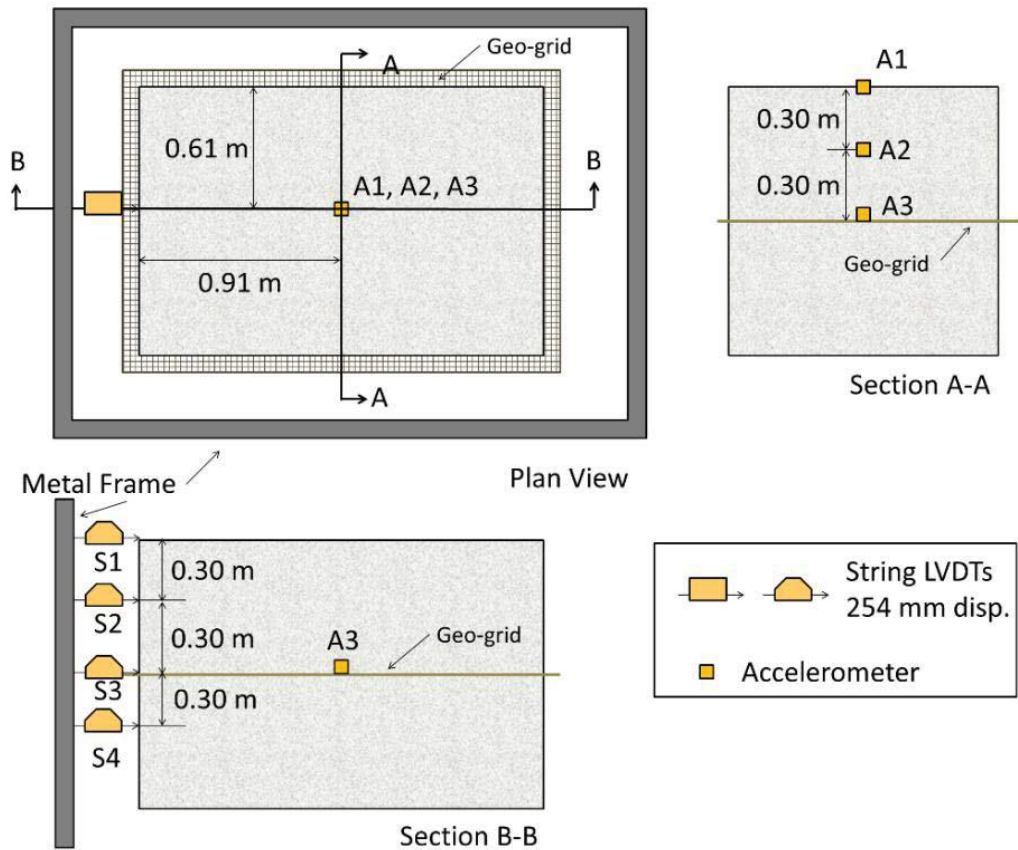


Figure 29: Experimental set-up for shake table modeling (copied from Tiwari et al., 2018c and 2018d)

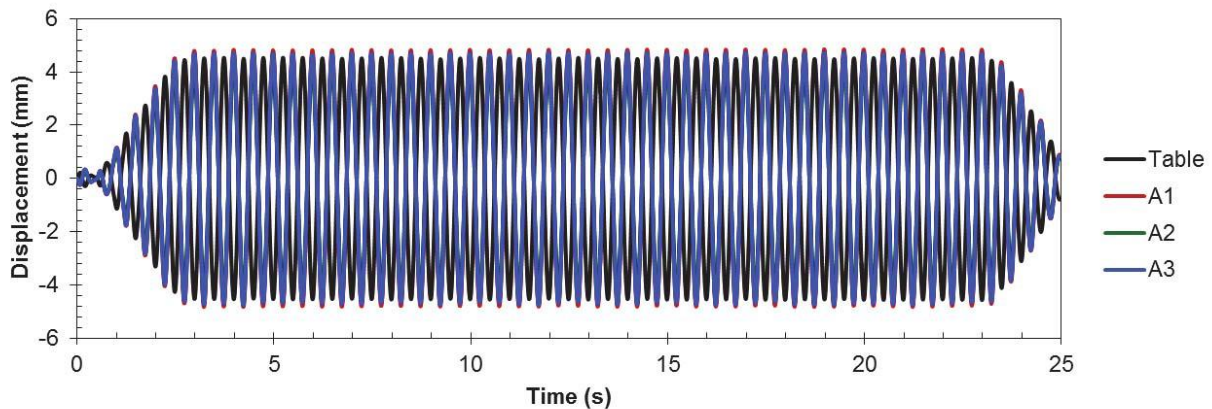


Figure 30: Displacement time histories in LCC retaining wall model with total equivalent height of 4.9 m subjected to sinusoidal cyclic loads with an amplitude of 0.1g at a frequency of 2 Hz reported by Tiwari et al. (2018c and 2018d)

Rollins et al. (2019) performed field tests to measure the passive resistance of a full-scale abutment wall with dense sand, controlled low-strength material (CLSM), and LCC

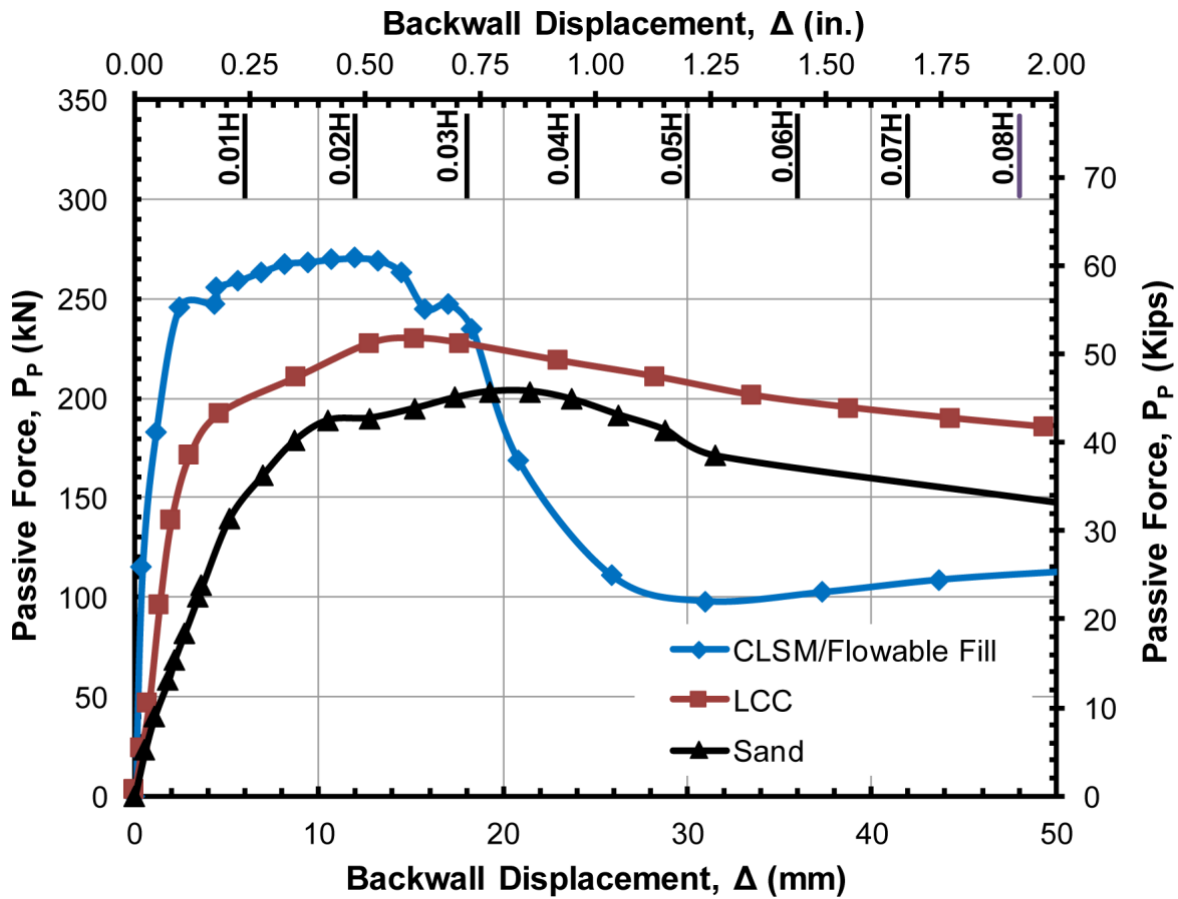


Figure 31: Results obtained by Rollins et al. (2019) (copied from Rollins et al, 2019)

Deni and Gladstone (2019) provided details of three case histories where LCC materials were effectively used for backfill of retaining walls on soft ground or flood plains (Figures 32 and 33). They mentioned the design methods they used for the MSE wall backfills; the walls were designed as a conventional MSE wall with backfill material having friction angle of 40 degrees (34 degrees minimum), as mentioned by Tiwari et al. (2017).

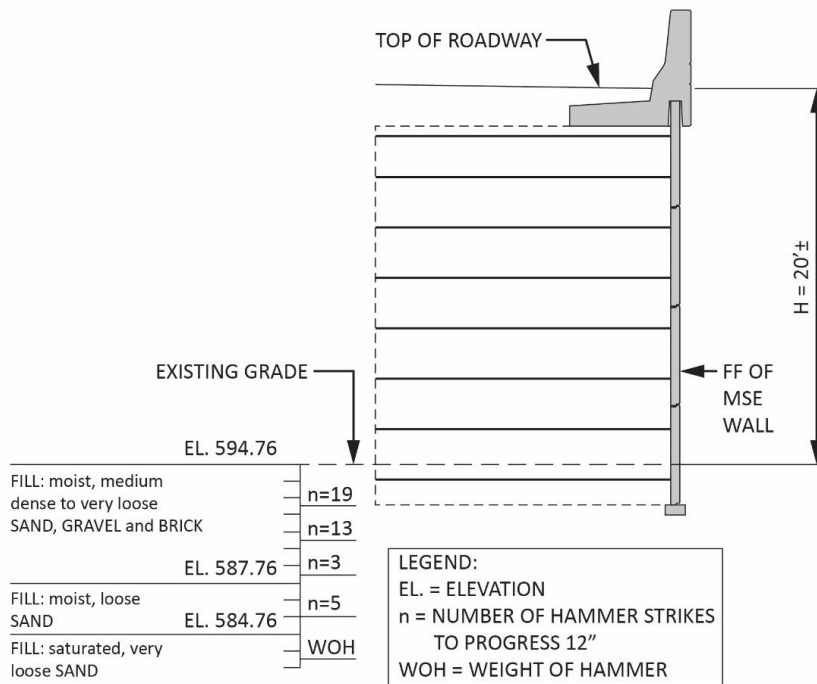
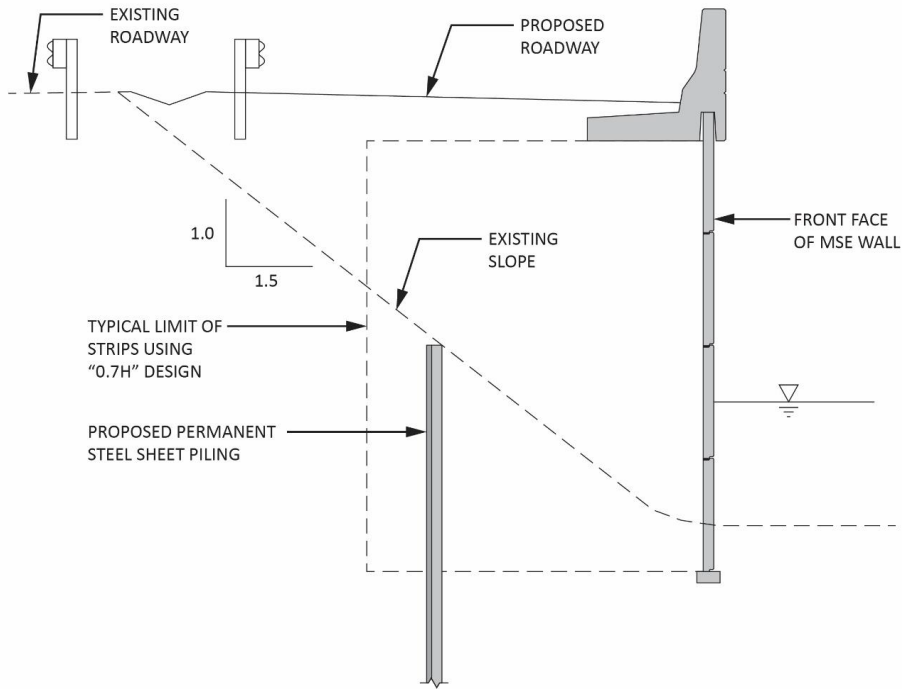


Figure 32: Cross-section of the Illinois DOT, I-64, St. Clair County LCC MSE wall designed by Deni and Gladstone (2019) (copied from Deni and Gladstone, 2019)

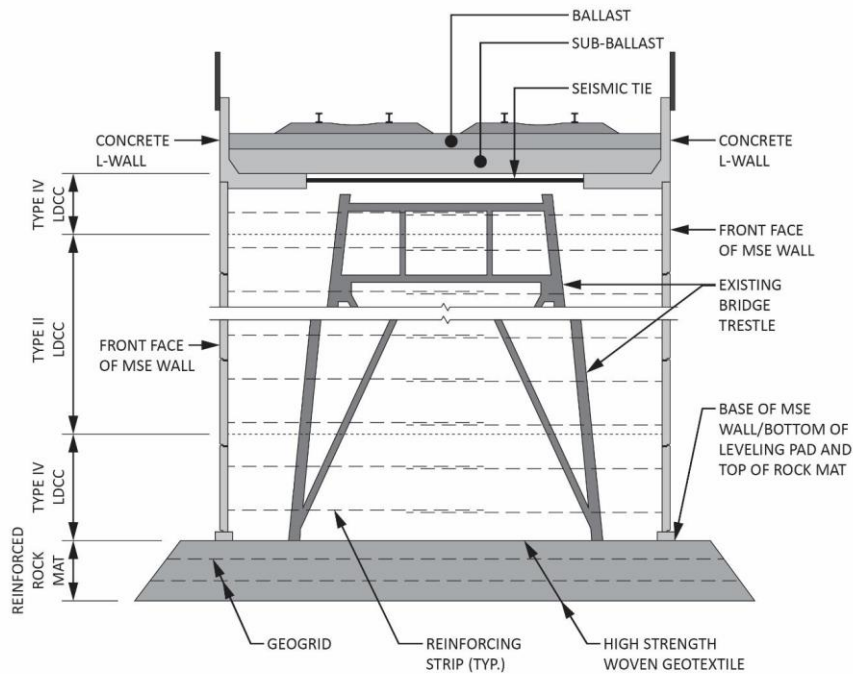


Figure 33: Cross-section of the Merchants Bridge Replacement over Mississippi River, St. Louis, MO LCC MSE wall designed by Deni and Gladstone (2019) (copied from Deni and Gladstone, 2019)

Anderson et al. (2012) designed an embankment with LCC material and estimated the seismic global stability of the embankment for Union Pacific railroad. They, with numerical analyses, concluded that the LCC material performs well during the design level earthquake.

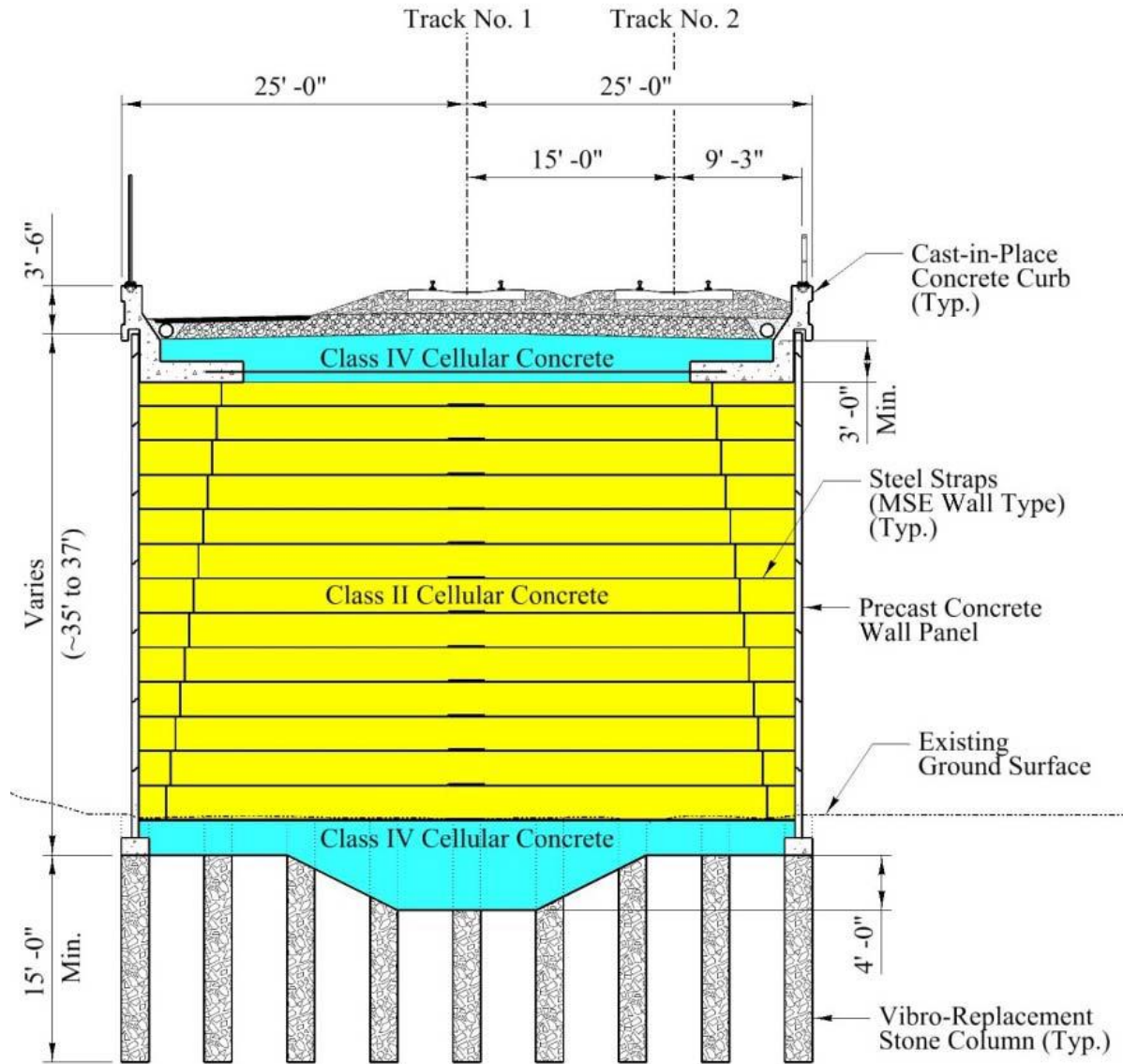


Figure 34: Cross-section of MSE wall designed by Anderson et al. (2012) (copied from Anderson et al, 2013). It was reported that Chimney Drains were used at both edges of the embankment for drainage.

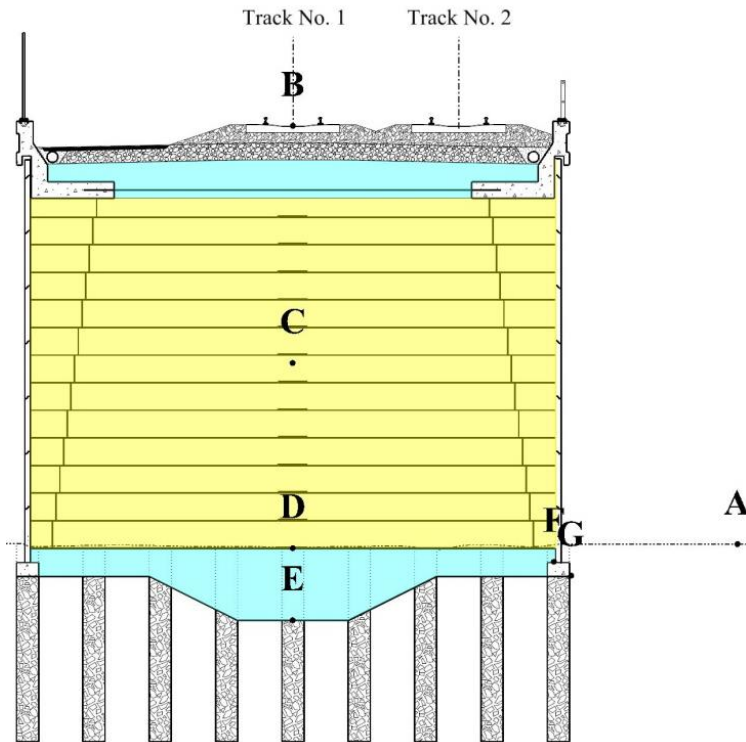


Figure 35: Seismic accelerations at different locations obtained by Anderson et al. (2012) (copied from Anderson et al., 2012). Table 2 shows the results.

Table 2 – Summary of Seismic Accelerations and Stresses at Level 3 Event

	History Point						
	A	B	C	D	E	F	G
X-Acceleration (%g)	1.72	1.48	1.19	0.98	0.97	0.97	0.97
Y-Acceleration (%g)	1.50	0.50	0.47	0.44	0.44	0.92	0.90
XY-Shear Stress (psf)	495	273	1607	1984	1789	4590	7315
X-Stress (psf)	693	275	196	816	1113	9296	10568
Y-Stress (psf)	712	263	1382	2058	2518	3460	12404

Considering all these discussions in the literature, it is important to study in detail regarding whether it is appropriate to LCC design retaining walls as rigid blocks/ panels or to follow the current practice to treat LCC as soil and use the MSE wall guidelines available in USA such as the one prepared by the CalTrans. However, there is a need of more studies to come up with the guideline pertinent to the design of LCC retaining walls if they are to be designed as rigid blocks. At present, conservative approach of designing the MSE wall with LCC material with 30 or 40° friction angle is considered a common practice as the current MSE wall design guideline uses only soil as the backfill material.

CASE STUDIES

For this study, the authors contacted over two dozen practitioners in USA who have been using LCC materials in geotechnical design of structures. All of them unanimously agreed that no significant distresses have been observed in the retaining walls, precast panels, and engineered fills. A few representative project details were also compiled for this study. Those projects are grouped based on their application as – a) annular grouting, b) precast panels, and c) lightweight fill grouting. Salient features of a few representative projects, among the collected information, are presented below. Please note that these projects are only examples and hundreds of projects, which are not included here, are now available throughout USA where LCC has been used in geotechnical structures.

1. *Annular Grouting*

Relining Los Angeles 90-Year Old Brick-lined Sewer (source: Cell-Crete Corporation)

Owner of this project is City of Los Angeles Public Works. This is a design-bid-build construction project that involved several contracts over the past 10 years in an attempt to reline 90-year old brick lined sewers in Los Angeles that are performing poorly due to age. New fiberglass circular and semi elliptical lining is being installed and grouted in place with LCC (Figure 36). There is little access as most of these sewers are located on the city's ROW with limited restriction from traffic and other utilities, however the ease of placement and small footprint of LCC mobile batch plants make the grouting installation reduce the traffic impact to the construction area. Another design consideration of grouting a live sewer line is the ability to control the flow in the pipeline and keep the pipe from becoming buoyant during grouting.

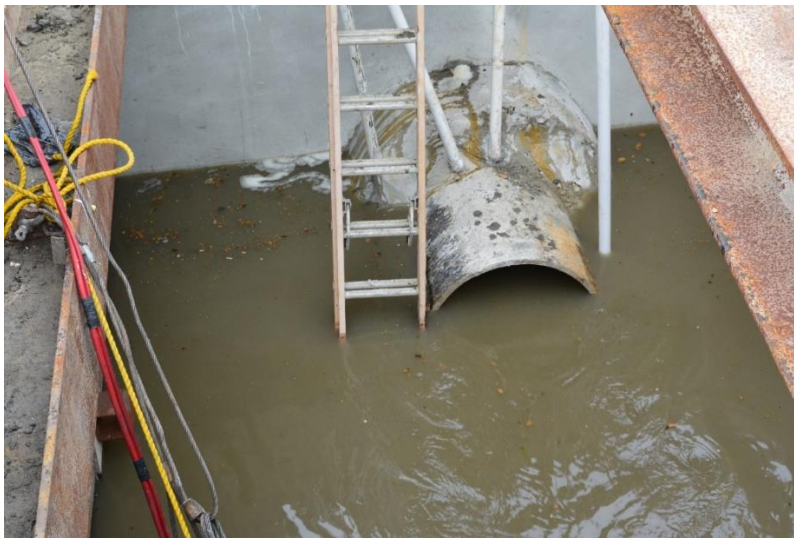


Figure 36. Annular grouting that relined 90-year old brick-lined sewer in Los Angeles (Source- Cell-Crete Corporation)

Pipeline 4 Relining at Lake Murray (Source: Cell-Crete Corporation)

Owner of this project is San Diego Water Authority. This is a design-bid-build construction project that has been ongoing. The city has issued several contracts to reline over 20 miles of existing waterline pre-stressed concrete cylinder pipes (PCCP). Waterline is set to be relined with new collapsible steel lining; the steel liner is placed in segments and welded together inside of the pipe (Figure 37). A small annular space is left behind. Intimate contact between host pipe and carrier pipe is required, LCC is being used to fill the annular space that varies from 1.5 to 3 inches. Grouting is taking place from inside the pipeline through grout ports prefabricated in the steel liner.



Figure 37. Relining pipeline at Lake Murray (Source: Cell-Crete Corporation)

2. Precast Segmental Retaining Wall with LCC Backfill

Bay Park Pinole (Source: Cell-Crete Corporation)

The owner of this project was Holiday retirement Corp. This was a design-build project that was required due to a heavy rainfall event that washed away a significant portion of

the hillside near an existing retirement facility, in Pinole, CA. The hillside slid away from the building and removed a large section of parking lot with it. As an effort to stabilize the area, LCC was proposed as a lightweight fill material which would reduce the risk of any future rainfall events from causing another slide. This project includes a 30 ft wide, 23 ft tall, and total of 171.5 ft long road expansion with new soil nail wall (Figure 38). A segmental block wall with geo-grids at 2 ft 8 in c/c was used. The project included 2 ft thick compacted subbase and pavement over the cellular concrete. A face panel is supported on micro-pile foundation and anchors, and cellular concrete 45 pcf and 300 psi UCS concrete is being used for the backfill material. The final depth of LCC fill was 21 ft, achieved in 2-3 ft lifts over the course of 9 days. The design approach for this project included treating the LCC material as embankment material and designing as a traditional / typical length MSE wall reinforcement and segmental retaining wall. Type of Reinforcement used was biaxial geogrid. No observed performance issues or concerns have been reported to date.



Figure 38 A section of the Bay Park Pinhole slide remediation project (Source: Cell-Crete Corporation).

Crenshaw Corridor/ LAX Transit Project (Source: Cell-Crete Corporation)

The owner of this project was METRO. This was a design build contract; LCC was selected for this project because there was a unreinforced concrete encasement for DWP Ductbanks running directly under new proposed embankment and were susceptible to settlement/cracking caused by increase in vertical pressure applied by additional fill load of new embankment supporting Metro's track ROW. As a solution to this problem, a low-density fill material in between MSE walls was chosen as the backfill material (Figure 39). The LCC substantially reduced the fill loads on the ductbanks and eliminated the potential for damage/settlement to the underground existing DWP lines. The design approach for this project included treating the LCC material as embankment material and designing as a traditional / typical length MSE wall reinforcement and segmental retaining wall. Type of Reinforcement used was steel ribbed strips by Reinforced Earth Company (RECo). No observed performance issues or concerns have been reported to date.



Figure 39 LCC material used for the Crenshaw Corridor/ LAX Transit project (Source: cell-Crete Corporation)

Gerald Desmond Bridge (Source: Cell-Crete Corporation)

The owner of this project is the Port of Long Beach. This is a design build project. LCC was chosen on this project due to the presence of compressible material on the East Side approaches to the bridge to address settlement and stability consideration on the in-situ soils and the magnitude of the design earthquake. A total of over 200,000 yard³ of the LCC materials have been placed on the project in 6 different locations using precast panels and LCC as the backfill material. Class II and Class III materials are being utilized on the east side approaches to the bridge (Figure 40). Class II LCC will be poured at the lower portions of a fill to maximize the load reduction, and Class IV LCC will be used at the uppermost layers directly under the pavement section. For this project, the design approach included treating the LCC material as an embankment material and designing the structure as a traditional / typical length MSE wall reinforcement. The type of reinforcement used was steel ladder reinforcement and ribbed steel straps. No observed performance issues or concerns have been reported to date.

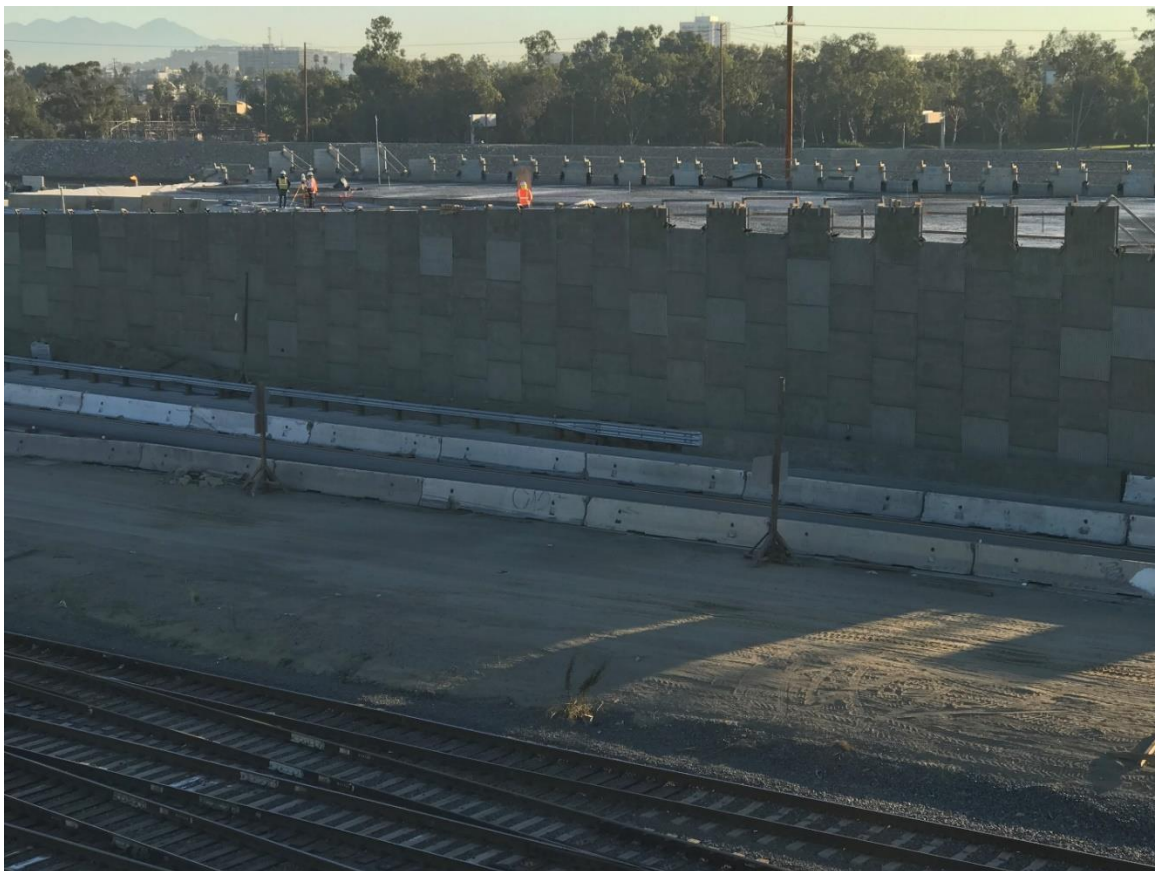


Figure 40 LCC MSE wall at Gerard Desmond Bridge project (Source: Cell-Crete Corporation)

Colton Crossing (Source: Cell-Crete Corporation)

The owner of this project was UPRR. This was a design bid project requiring a 8150 ft of flyover structure to be built to alleviate the bottleneck created by the intersection of UPRR and BNSF tracks in the area (Figure 41). Minimal interruption to the track, the proximity to the 10 freeway, a small construction footprint area and soft soils found in the area required an innovative construction solution to solve these issues and increase the feasibility of this complex project. LCC offered the exact solution to this project although it had not been used before in this quantity or height. The LCC eliminated the need for conventional RW structures and also assisted with overburden pressure on soft soils and reduced the impact on design in an area know for its high seismic activity due to the low density of this backfill material. Two mobile batch plants were able to produce over 2,000 yard³ a day of material and placed a total of 220,000 yard³ material, the largest placement to date back in 2007. No observed performance issues or concerns have been reported to date.



Figure 41 LCC MSE wall constructed at Colton Crossing (Source: Cell-Crete Corporation).

Lynn Center Bridge Replacement: Henry County, IL (Source: Aerix Industries)

Home to one of BNSF's major railroads, Lynn Center is a small community in Henry County, Illinois that plays a big role in the transportation of freight across North America. Therefore, when the bridge that spanned the BNSF railroad at Lynn Center began to show signs of deterioration, the Illinois Department of Transportation (DOT) needed to act quickly. This bridge replacement project consisted of a number of steps and required particular attention to detail in engineering design, scheduling, and selection of construction materials. The construction of the bridge abutments was one of the first steps in this project, and the selection of a strong, lightweight fill material was essential for this construction. National contractor Geo-Cell Midwest LLC chose to use a non-pervious low-density LCC for this portion of the project. The material chosen not only needed to be lightweight to reduce lateral and loads on abutment walls, but also needed to provide superior compressive strength, as it would have to withstand the placement of a 120-ton crane on top of the abutments for the bridge beam placement that would follow. Once the concrete abutment walls were formed and cast in place, the three-person construction crew from Geo-Cell Midwest installed LCC for each bridge abutment, using four-foot lifts (Figure 42). The LCC installation was completed in five short days.



Figure 42 MSE wall built at Lynn Center Bridge Replacement project (Source: Aerix Industry)

Roosevelt Avenue Bridge - Flushing, NY (Source: Aerix Industries)

The Roosevelt Avenue Bridge in Flushing, NY has been carrying New York City commuters and area residents for more than 80 years. When it was built in 1927, this bridge was the largest double-leaf bascule moveable bridge in the world. This multi-deck bridge now carries four lanes of Roosevelt Avenue vehicular traffic, two sidewalks and three tracks of the Interborough Rapid Transit Company (IRT) 7 line of the New York City subway. In January 2010, after decades of wear and tear, the bridge was showing signs of deterioration, and the NYC Department of Transportation (DOT) decided to start a \$60 million rehabilitation project. This entire rehabilitation project would include replacing the bridge's road deck, repainting and repairing the steel truss, approach structures, and repairing the bridge's concrete structure. In addition, the eight-foot sidewalks would be widened to 10 feet, and bike lanes would be included. A large portion of this project, requiring 1% of the \$60 million budget, entailed filling the voids of the abandoned counterweight well pits of the original drawbridge structure. This was a complex portion of the project that required a unique fill material that would be able to withstand not only the weight of the structure, but also the vibrations caused by the train and vehicular traffic that travelled over the bridge during the installation process. Specifications required that the fill material also provide a density equal to or less than that of water. The contracted installer installed 7,000 cubic yards of the LCC into the 29-foot-high well pits of the drawbridge (Figure 43).



Figure 43: LCC material used in the Roosevelt Avenue Bridge (Source: Aerix Industries)

SR-154 at Redwood Road; Interchange (Source: Gerhart Cole Inc.)

Owner of this project is Utah Department of Transportation (UDOT) and it is a design-build grade separation interchange project initiated in 2014. The fill heights were up to 25 feet and the walls lengths were up to approximately 500 feet. The main purpose of this project was to reduce load / vertical effective stresses below yield stress (i.e. maximum past pressure) at depth in fine-grained layer(s). In this project, the MSE wall footprint was over-excavated and replaced with MSE wall backfill with LCC (Figure 44). The use of LCC accelerated construction schedule and reduced the risk of excessive long-term settlements. For this project, the design approach included designing the LCC as an embankment and designing the wall structure as a traditional / typical length MSE wall reinforcement. The type of reinforcement used was ribbed metallic straps. No performance issues or concerns have been reported to date.



Figure 44 MSE Wall constructed for the SR-154 project (Source: Gerhart Cole Inc.)

I-15; SR-73 to 12300 South Widening (Source: Gerhart Cole Inc.)

Owner of this project is also Utah Department of Transportation (UDOT). This is a design-build roadway widening project initiated in 2015. This project involved a roadway widening near a large existing / historic utility vault. The fill heights were up to 12 feet and the walls length extended up to approximately 100 feet (Figure 45). In this project also, the MSE wall footprint was over excavated and replaced with an MSE wall backfill with LCC. This reduced load / earth pressures on the existing utility vault and eventually reduced costs by eliminating vault / utility line replacement and relocation. This also simplified utility agreements and coordination. The design approach for this project included treating the LCC material as embankment material and designing as a traditional / typical length MSE wall reinforcement with segmental retaining wall facing. Type of reinforcement used was biaxial geogrid. No observed performance issues or concerns have been reported to date.

Figure 45 illustrates the construction and wall conditions in January 2019



Figure 45 – Overview of the LCC MSE wall at I-15; SR-73 project. (Source: Gerhart Cole Inc.)

LCG Columbia Storage Project (Source- Cell-Crete Corporation)

The LCG Columbia Storage project is located in the city of Portland Oregon. When it is complete, it will be the largest self-storage unit in the Pacific Northwest. Over the course of the project, Cell-Crete will pour 7500 cubic yards of 27 psf concrete. This will be done in two phases, with phase one almost complete and phase two beginning in spring of 2020. Figure 46 shows some locations where the LCC materials are placed.

Along with its size, the location possesses its own set of challenges. The pour area has a 45-degree slope that makes it difficult for the crew to navigate, and also makes calculating take offs and building bulkheads more of a challenge. Through these challenges, the crew has done a great job of keeping production up and maintaining a positive mentality.



a



b

Figure 46 a and b – Overview of the LCC placement at the LCG Columbia Storage project.
(Source: Source- Cell-Crete Corporation)

OC 405 – LCC (Source – Cell-Crete Corporation)

LCC is being used on the project on over 50 bridge approaches, roadway fills, freeway widening, pipeline abandonment and many other applications. The bulk of the material will be placed over soft clay soils (Figure 47) to reduce fill loading eliminating the inadequate factor of safety against bearing capacity failure and reducing the load induced settlements, this project will require over 200,000CY of material and the project is scheduled to be completed in 2024.



a



b



c

Figure 47 a, b, and c – Overview of the OC 405 LCC project where LCC materials will be placed (Source: Source- Cell-Crete Corporation)

25th Ave. Grade separation (Source: Throop Lightweight Fill)

Figure 48 shows the photograph of 25th Avenue grade separation project, provided by the Throop Lightweight Fill. Throop Lightweight Fill can be contacted for further design details of the project. While the project is still ongoing, there were also no observed performance issues reported for this project after the completion of the LCC installation of the project.



Figure 48 Overview of 25th Avenue Grade Separation project (Source: Throop Lightweight Fill)

3. Lightweight Fill Grouting

Los Angeles Stadium and Entertainment District at Hollywood Park (Source: Cell-Crete Corporation)

This is a privately-owned project. Due to FAA regulations the new LA stadium could not exceed certain building height limits. A mass 120 ft deep excavation took place to accommodate the stadium without infringing on FAA regulation. Due to seismic considerations the stadium was built around a MSE wall “moat” that would allow the stadium to move during a seismic event without damaging the structure. The MSE wall was over 100 ft, the tallest in the country and the engineers were worried about the additional overburden pressure from fill load above the MSE walls to build canyon walls up to finished grade (Figure 49 and 50). LCC, class II, was used to reduce the overall fill loads on top of the MSE wall; over 130,000 yard³ of material was placed on the East, West and North Canyon walls in addition to being placed around the isolation casings for the roof structure.

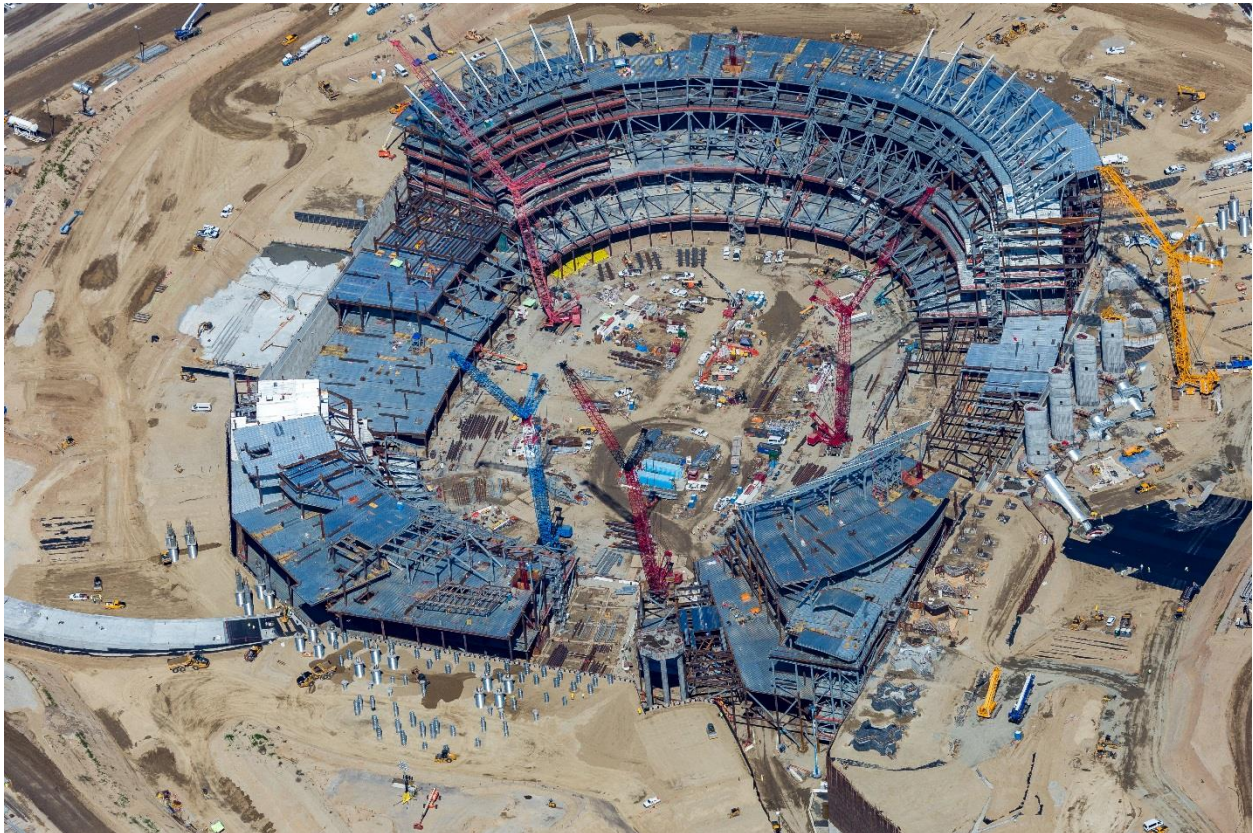


Figure 49 Overview of the LCC locations on the east west and north of the stadium constructed at Los Angeles Stadium (Source: Cell-Crete Corporation)



Figure 50 Closed view of the LCC at the Los Angeles Stadium (Source: Cell-Crete Corporation)

SUMMARY AND CONCLUSION

LCC materials have been used extensively in the past 60 years for various engineering applications such as insulation, light weight engineered fill, annular grout filling, and retaining walls. However, there are very limited data and design methods available pertinent to the physical and mechanical properties of the LCC materials. Moreover, it has been almost 15 years since the past standard has been published for the LCC materials lighter than 50 ft³. This article contains an extensive review of the properties as well as current applications of LCC materials in engineering practice. Although this material has been heavily used in practice for various geotechnical engineering applications such as MSE wall backfills, there is no standard available in practice to design MSE walls using the LCC materials. As such, conservative methods have been used to design the MSE wall backfill, ignoring the cohesion of the material as the current practice requires this material to be treated as soil. However, as the LCC material has high cohesion an appropriate guideline is needed for the design of retaining walls using the LCC material.

It is to be noted that most part of this material, specifically example projects, excludes the LCC materials heavier than 50 pcf and pervious LCC material as that was out of scope of this project.

ACKNOWLEDGEMENT

The authors would like to thank the California Nevada Cement Association for the opportunity to compile the state-of-the-practice information, some of the data presented in this article and financial support to generate this report. Moreover, the authors would like to thank Cell-Crete Corporation, Throop Lightweight Fill, Aerix Industries, and Gerhart Cole, Inc (Ryan Maw and Ryan Cole) for providing description of the projects and the figures presented in this article. The authors would like to thank Dr. Beena Ajmera, Assistant Professor of Civil and Environmental Engineering at North Dakota State University for her help during literature collection.

REFERENCES:

1. ACI 213 R-87 (1999), Guide for Structural Lightweight (Reapproved Aggregate Concrete
2. Aerix Industries
3. American Concrete Institute (2006), Guide for Cast-in-Place Low-Density Cellular Concrete, ACI 523.1R-06, 1-13.
4. American Concrete Institute (2014), Guidance for Cellular Concrete above 50 pcf, ACI 523.3R-14, 1-17.
5. Amran, Y.H.M., Farzadnia, N., and Ali, A.A.A. (2015), Properties and application of foamed concrete; a review, *Construction and Building Materials*, 101, 990–1005.
6. Anderson, J., Bartlett, S., Dickerson, N., and Poepsel, P., (2012). “Development of Seismic Design Approach for Freestanding Freight Railroad Embankment Comprised of Lightweight Cellular Concrete”, in *State of the Art and Practice in Geotechnical Engineering*, ASCE 2012 Geo-Congress, Oakland, CA., 1720-1729.
7. ASTM C495 / C495M - 12 (2012), Standard Test Method for Compressive Strength of Lightweight Insulating Concrete.
8. ASTM C666 / C666M - 15 (2015), Standard Test Method for Resistance of Concrete to Rapid Freezing and Thawing.
9. ASTM D2434-68 (2006), Standard Test Method for Permeability of Granular Soils (withdrawn in 2015)
10. ASTM D4644 - 16 (2016) Standard Test Method for Slake Durability of Shales and Other Similar Weak Rocks
11. Brady, K.C., Watts, G. R. A., and Jones, M. R. (2001). Specification for foamed concrete, Prepared for Quality Services, Civil Engineering Highways Agency, Application Guide AG39, TRL Limited.
12. CalTrans (2014): Caltrans Geotechnical manual: Ground Improvement, 1-21.
13. Cell-crete Corporation
14. Chandra, S., and Brentsson, L. (2003). *Lightweight aggregate concrete science, technology and applications*, Standard Publisher Distributors, Göteborg, Sweden.
15. ENGEO/CNCA (2016), CNCA Cellular Concrete testing, Report submitted to California Nevada Cement Association.
16. Deni, N., and Gladstone, R.A., (2019) *Low-Density Cellular Concrete in MSE Structures with Steel Strip Reinforcements—Design and Construction Considerations and Case Histories*, Geotechnical Special Publication, 306, 127-139
17. *Engineered Fill* (2011), Elastizell EF (Engineered Fill) Geotechnical Applications, Elastizell Corp., 16 pp.
18. Gerhart Cole Inc.
19. Gerhart Cole Inc. (2015), Cellular Concrete Laboratory testing program, Laboratory Testing Observations and Results, Cell-crete Corporation.

20. Hilal, A.A., Thoma, N.H., and Dawson, A.R. (2015), On void structure and strength of foamed concrete made without/with additives, *Construction and Building Materials*, 85, 157–164.
21. Hoff, G.C. (1970a), Low Density Concrete Backfill for Lined Tunnels, ACI Special Publication SP 29: Lightweight Concrete, American Concrete Institute, 221-251.
22. Hoff, G.C. (1970b), New Application for Low-density Concrete, ACI Special Publication SP 29: Lightweight Concrete, American Concrete Institute, 181-219.
23. Hoff, G.C. (1972), Porosity – Strength Consideration for Cellular Concrete, US Army Corp of Engineers, Miscellaneous Paper C-72-1
24. Legatski, L.A. (1994), Chapter 49: Cellular Concrete, Significance of Tests and Properties of Concrete and Concrete Making Materials, ASTM STP 169C, ASTM International., 533-539.
25. Maruyama, R. C., and Camarini, G. (2015). “Properties of cellular concrete for filters.” *IACSIT Int. J. Eng. Technol.*, 7(3), 223–228.
26. Pradel, D., and Tiwari, B. 2015. The use of MSE walls backfilled with Lightweight Cellular Concrete in soft ground seismic areas, *Proceedings of the 3rd International Conference of Deep Foundations*, 1, 107-114.
27. Rahman, M.Z.A.A., Zaidi, A.M.A., and Rahman, I.A. (2010), Physical Behavior of Foamed Concrete under uniaxial compressive load: confined compressive tests, *Modern Applied Science*, 4 (2), 126-132.
28. Ramamurthy, K., Nambiar, E.K.K., and Ranjani, G.I.S., (2009), A classification of studies on properties of foam concrete, *Cement & Concrete Composites*, 31, 388–396.
29. Reichard, T.W. (1970), Mechanical Properties of Insulating Concrete, ACI Special Publication SP 29: Lightweight Concrete, American Concrete Institute, 253-317.
30. Rollins, K., Wagstaff, K.B., and Black, R. (2019), Passive Force-Deflection Curves for Controlled Low-Strength Material (CLSM) and Lightweight Cellular Concrete (LCC), *Geotechnical Special Publication*, 306, 119-126
31. Tiwari, B. (2015), Static and Dynamic Properties of LDCC Materials, Cell-crete Corporation.
32. Tiwari, B. (2018), Seismic Deformation of LDCC Material on shake table modeling, Cell-crete Corporation.
33. Tiwari, B., Ajmera, B., Maw, R., Cole, R., Villegas, D., and Palmerson, P. (2017), Mechanical Properties of Lightweight Cellular Concrete for Geotechnical Applications, *Journal of Materials in Civil Engineering*, ASCE, 29 (7), 06017007 1-7.
34. Tiwari, B., Ajmera, B., Maw, R., Cole, R., Villegas, D., and Palmerson, P. (2018a) Closure to “Mechanical Properties of Lightweight Cellular Concrete for Geotechnical Applications by Binod Tiwari, Beena Ajmera, Ryan Maw, Ryan Cole, Diego Villegas, and Peter Palmerson, *Journal of Materials in Civil Engineering*, 30(9), 07018004 1-2.

35. Tiwari, B., Ajmera, B., and Villegas, D. (2018b), Dynamic Properties of Lightweight Cellular Concrete for Geotechnical Applications, *Journal of Materials in Civil Engineering*, 30 (2), 04017271 1-10.
36. Tiwari, B., Ajmera, B., and Villegas, D. (2018c). "Cyclically Induced Deformations in Lightweight Cellular Concrete Backfilled Retaining Structures," *Proceedings of the International Foundations Conference and Equipment Expo 2018 Geotechnical Special Publication* 297, 130-138.
37. Tiwari, B., Ajmera, B., and Villegas, D. (2018d). "Dynamic Response of Lightweight Cellular Concrete MSE Walls," *Proceedings of GeoShanghai 2018*, 6, 168-175.
38. Towery, T. (2018), Discussion of Mechanical Properties of Lightweight Cellular Concrete for Geotechnical Application by Tiwari et al. (2017), *Journal of Materials in Civil Engineering*, 30(9), 07018003-1-2.
39. Valore RC. (1954), Cellular concrete part 1 composition and methods of production, *ACI J*; 50:773-96.
40. Wei, S., Yiqiang, C., Yunsheng, Z., and Jones, M.R. (2013), Characterization and simulation of micro-structure and thermal properties of foamed concrete, *Construction and Building Materials*, 47, 1278-1291.
41. Zhihua, P., Hengzhi, L., and Weiqing, L. (2014), Preparation and characterization of super low density foamed concrete from Portland cement and admixtures, *Construction and Building Materials*, 72, 256-261.